Accepted Manuscript

Design, synthesis and evaluation of novel diaryl-1,5-diazoles derivatives bearing morpholine as potent dual COX-2/5-LOX inhibitors and antitumor agents

Zhang Li, Zhong-Chang Wang, Xin Li, Muhammed Abbas, Song-Yu Wu, Shen-Zhen Ren, Qi-Xing Liu, Yi Liu, Peng-Wen Chen, Yong-Tao Duan, Peng-Cheng Lv, Hai-Liang Zhu

PII: S0223-5234(19)30219-3

DOI: https://doi.org/10.1016/j.ejmech.2019.03.008

Reference: EJMECH 11178

To appear in: *European Journal of Medicinal Chemistry*

Received Date: 19 November 2018

Revised Date: 4 March 2019

Accepted Date: 4 March 2019

Please cite this article as: Z. Li, Z.-C. Wang, X. Li, M. Abbas, S.-Y. Wu, S.-Z. Ren, Q.-X. Liu, Y. Liu, P.-W. Chen, Y.-T. Duan, P.-C. Lv, H.-L. Zhu, Design, synthesis and evaluation of novel diaryl-1,5-diazoles derivatives bearing morpholine as potent dual COX-2/5-LOX inhibitors and antitumor agents, *European Journal of Medicinal Chemistry* (2019), doi: https://doi.org/10.1016/j.ejmech.2019.03.008.

Design, synthesis and evaluation of novel diaryl-1,5-diazoles derivatives bearing morpholine as potent dual COX-2/5-LOX inhibitors and antitumor agents

Zhang Li[a,†], Zhong-Chang Wang [a,†,*], Xin Li [a], Muhammed Abbas, Song-Yu Wu[a], Shen-Zhen Ren [a], Qi-Xing Liu [a], Yi Liu [a], Peng-Wen Chen [b], Yong-Tao Duan[c], Peng-Cheng Lv [a,*], Hai-Liang Zhu [a,*]

[a] *State Key Laboratory of Pharmaceutical Biotechnology, Nanjing University, Nanjing 210023, PR China*

[b] *School of Chemistry and Chemical Engineering, Nanjing University, Nanjing 210023, PR China*

[c] *Henan Provincial Key Laboratory of Children's Genetics and Metabolic Diseases, Zhengzhou Children's Hospital, Zhengzhou 450018, PR China*

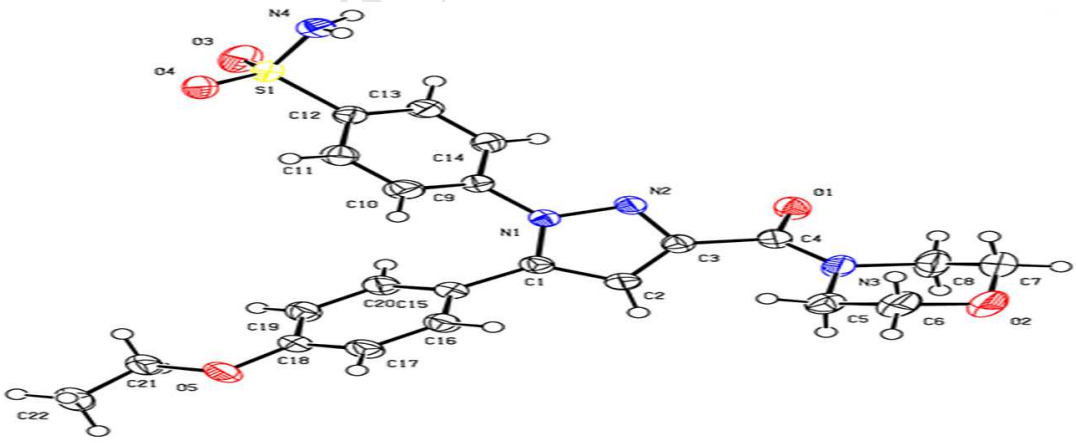

A series of novel dual COX-2/5-LOX inhibitors have been synthesized and evaluated for their anti-cancer activity as potential COX-2/5-LOX inhibitors. Compound **A33** was the most active.

Design, synthesis and evaluation of novel diaryl-1,5-diazoles derivatives bearing morpholine as potent dual COX-2/5-LOX inhibitors and antitumor agents

Zhang Li[a,†], Zhong-Chang Wang [a,†,*], Xin Li [a], Muhammed Abbas, Song-Yu Wu[a], Shen-Zhen Ren [a], Qi-Xing Liu [a], Yi Liu [a], Peng-Wen Chen [b], Yong-Tao Duan[c], Peng-Cheng Lv [a,*], Hai-Liang Zhu [a,*]

[a] *State Key Laboratory of Pharmaceutical Biotechnology, Nanjing University, Nanjing 210023, PR China*

[b] *School of Chemistry and Chemical Engineering, Nanjing University, Nanjing 210023, PR China*

[c] *Henan Provincial Key Laboratory of Children's Genetics and Metabolic Diseases, Zhengzhou Children's Hospital, Zhengzhou 450018, PR China*

Declarations of interest: none

*Corresponding author. Tel. & fax: +86-025-89682572; e-mail: wangzhongchang2006@163.com (WZC), zhuhl@nju.edu.cn (ZHL), pengcheng.lui@gmail.com (LPC)

†These two authors equally contributed to this paper.

Abstract:

In this paper, 41 hybrid compounds containing diaryl-1,5-diazole and morpholine structures acting as dual COX-2/5-LOX inhibitors have been designed, synthesized and biologically evaluated. Most of them showed potent antiproliferative activities and COX-2/5-LOX inhibitory *in vitro*. Among them, compound **A33** displayed the most potency against cancer cell lines (IC_{50} = 6.43-10.97 μM for F10, HeLa, A549 and MCF-7 cells), lower toxicity to non-cancer cells than celecoxib (**A33**: IC_{50} = 194.01 μM *vs.* **celecoxib**: IC_{50} = 97.87 μM for 293T cells), and excellent inhibitory activities on COX-2 (IC_{50} = 0.17 μM) and 5-LOX (IC_{50} = 0.68 μM). Meanwhile, the molecular modeling study was performed to position compound **A33** into COX-2 and 5-LOX active sites to determine the probable binding models. Mechanistic studies demonstrated that compound **A33** could block cell cycle in G2 phase and subsequently induced apoptosis of F10 cells. Furthermore, compound **A33** could significantly inhibit tumor growth in F10-xenograft mouse model, and pharmacokinetic study of compound **A33** indicated that it showed better stability *in vivo*. In general, compound **A33** could be a promising candidate for cancer therapy.

Keywords: diaryl-1,5-diazoles, morpholine, cyclooxygenase-2, 5-lipoxygenase, anticancer

1. Introduction:

Inflammatory response exhibited pleiotropic effects in the development of cancer. On one hand, inflammation contributes to carcinogenesis, tumor growth, invasion, metastatic spread, and malignant transformation. On the other hand, it also stimulates immune effector mechanisms that might limit tumor growth [1]. However, numerous studies have proved that chronic inflammation is generally detrimental and can increase the risk of cancer[2-3]. And tumor micro-environments contain various inflammatory mediators, such as cytokines, chemokines and growth factors, which accelerate extravasations of tumor cells through the stroma and promote the development of carcinogenesis by participating in complex signaling processes[4]. Thus, targeting these factors associated with inflammation in cancer cells can offer rational treatment strategies for cancer.

The potent inflammation mediators are derivatives of arachidonic acid (AA) a poly-unsaturated fatty acid produced from membrane phospholipids. AA metabolism includes two principal pathways, one is the cyclooxygenase (COX) pathway, which converts AA to prostaglandins (PGs) and thromboxanes (TXs); the other is lipoxygenase (LOX) pathway, which produces a collection of leukotrienes (LTs) and hydroxyeicosatetranoic acids (HETEs)[5-6]. It is well known that COX exists in two isoforms COX-1 and COX-2, among which COX-1 is a constructive enzyme found in most normal tissues as a “house-keeper” one, while COX-2 is an inducible enzyme found in macrophages, fibroblasts and leukocytes, and is up-regulated in a variety of tumor types[7-9]. 5-LOX, a human non-heme enzyme, is a vital member of LOXs and

responsible for the production of leukotriene B_4 (LTB_4) and 5-HETE, which could enhance cell proliferation, inhibit apoptosis, and promote cancer development[10-11].

The over-expression and activities of COX-2 and 5-LOX in tumor cells are closely related to cell cycle, blocking apoptosis and stimulating angiogenesis. Lots of results indicated that elevated levels of COX-2 and 5-LOX would result in elevation of downstream prostaglandin E_2 (PGE_2) and LTB_4 levels respectively[12]. PGE_2, a major inflammation mediator with meaningful biological functions, could increase the motility and metastatic potential of tumor cells, promote tumor angiogenesis, induce local immunosuppression and suppress apoptosis[13-14]. Meanwhile, COX-2 itself could promote tumor cells survival by lowing the levels of unesterified AA, and COX-2 peroxidase has also been shown to convert many procarcinogens into ultimate carcinogens, thereby promoting the deterioration of tumors[15-16]. Given the previous research, COX-2 and 5-LOX with strikingly similar biological functions are frequent co-expression. Inhibition of the COX pathway would switch AA metabolism to the LOX pathway and vice versa, resulting in elevated levels of leukotrienes or prostaglandins, which in turn cause fatal side effects[17]. Drugs acting on individual molecular targets would produce unfavorable activity, toxicity, and drug resistance, whereas drugs acting on multiple targets synchronously are less prone to drug resistance, reduce side effects, and better exert drug activity, produce better therapeutic effects[18]. It is believed that compounds which could inhibit COX-2/5-LOX concurrently would shut off the production of mediators of inflammation from the AA pathway. Thus dual COX-2/5-LOX inhibitors established a

worthy rational approach to obtain effective and safer anti-tumor agents.

Diaryl five-membered heteroatom system is a characteristic structure in numerous selective COX-2 inhibitors displaying higher COX-2 selectivity and better safety profile, such as **Celecoxib**, **Rofecoxib**, and **SC558**[19-21]. Meanwhile, structure activity relationship (SAR) studies of COX-2 indicated the significance of aminosulfonyl (SO_2NH_2) pharmacophore for COX-2 selectivity[22-23]. Furthermore, some antioxidant 5-LOX inhibitors such as **Phenidone** and **BW-755C** are comprised of pyrazole that the core pharmacophore which also appear to inhibit the COX isoforms[24-25]. The pharmacological effects of morpholine derivatives are of great significance in different biological fields. Emerging evidence demonstrated that morpholine and its analogs have shown favorable anti-inflammation, anti-cancer, anti-oxidant and anti-microbial activities[26], as well as reduced gastrointestinal and cardiovascular side effects[27-28]. For example, the *cis*-2,3-disubstituted morpholine **aprepitant 4** is used to treat nausea and vomiting caused by chemotherapy[29]. **Moroxydine**, a common morpholine-containing drug, is mainly used to treat viral influenza. The introduction of morpholine derivatives is expected to inhibit COX-2/5-LOX simultaneously, enhance physiological activities and reduce toxic side effects[30-31].

Over the past few years, we had reported a series of diarylpyrazole derivatives as selective COX-2 or dual COX-2/5-LOX inhibitors and successfully obtained some potent anticancer candidates[32-36]. Based on the above findings, a series of compounds incorporating diaryl-1,5-diazoles and morpholine pharmacophores were

designed and synthesized to explore more potent and safer dual COX-2/5-LOX inhibitors for anticancer candidates (**Figure 1**). Hereupon, the synthesis, *in vitro* and *in vivo* biological evaluation has been reported. Meanwhile, docking studies were performed to understand the possible models of the most potent compound **A33** into both COX-2/5-LOX active sites in order to explain their anti-cancer activities.

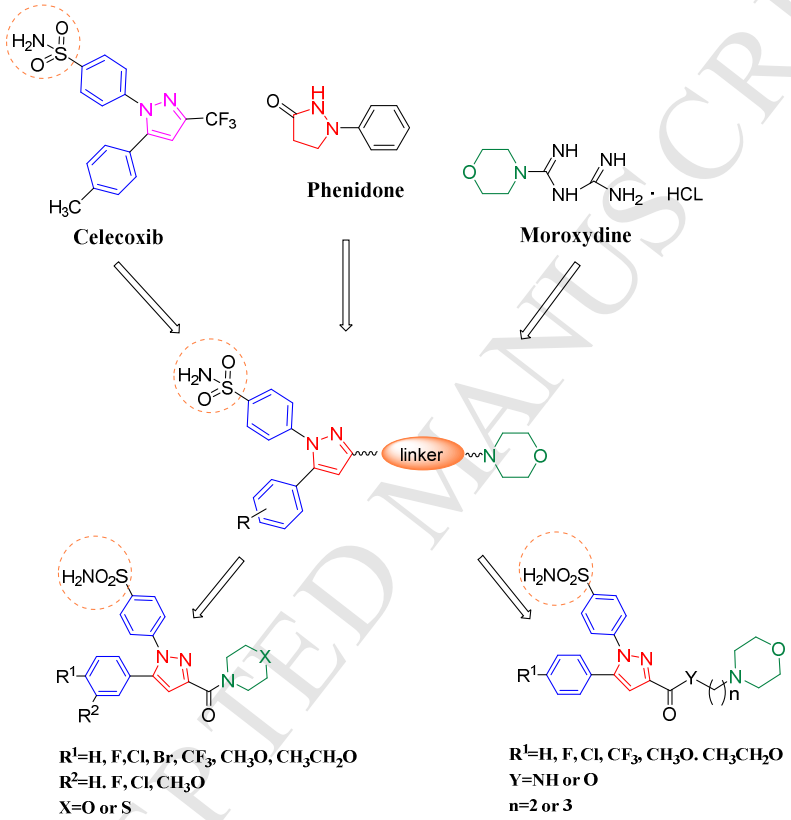

Fig 1. Structure of Celecoxib, Phenidone and Moroxydine and targeted compounds as dual COX-2/5-LOX inhibitors

2. Result and discussion

2.1 Chemistry

The synthetic route of starting materials **4a-4k** has been described in the previous study (**Scheme 1**)[36]. Catalyzed by excess sodium methoxide, the substituted acetophenone reacted with dimethyl oxalate to form diverse chalcones **2a-2k**, then

2a-2k were reacted with 4-hydrazinylbenzenesulfonamide to obtain the intermediate **3a-3k**. Finally, **3a-3k** were hydrolyzed by potassium hydroxide into corresponding pyrazolesulfonamide carboxylic acid **4a-4k**. The solvent used in the above three steps was methanol.

Scheme 1[a]

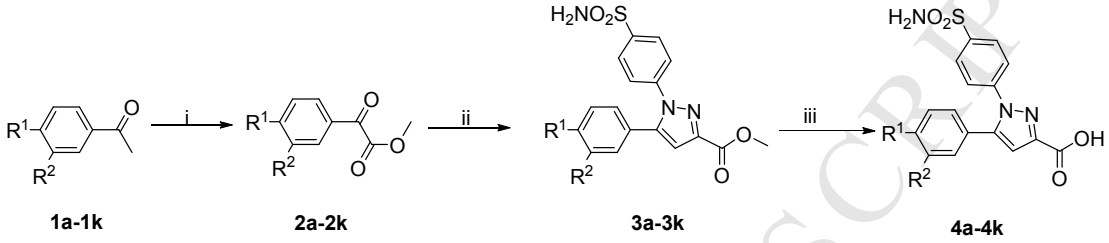

[a] Reagents and conditions: (i) dimethyl oxalate, methanol, reflux 6 h; (ii) 4-hydrazinylbenzenesulfonamide, methanol, reflux, 6 h; (iii) KOH, methanol, reflux, 2 h.

The synthesis of target compounds **A1-A41** was outlined in **Scheme 2** and **3**. The starting materials **4a-4k** were activated by EDC·HCl, HOBt and DMAP at 0 □ for half an hour, followed by esterification condensation reaction with different morpholine derivatives to form the corresponding target compound **A1-A41**. The purified compounds were prepared by subsequent column chromatography and crystallization. The structures of the target compounds **A1-A41** were shown in **Table 1** and **2**. All targeted compounds were first reported and characterized by ^{1}H NMR spectroscopy, ^{1}C NMR spectroscopy, melting point, ESI-MS and elemental analysis, in accordance with their depicted structures.

Scheme 2[a]

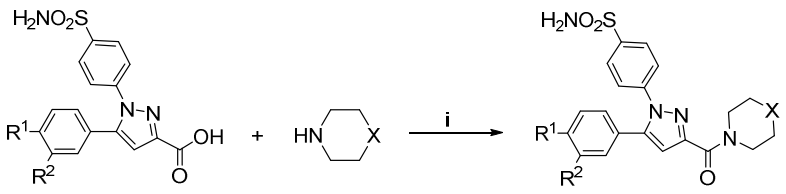

[a] Reagents and conditions: (i) EDC·HCl, HOBt, DMAP, dichloromethane, 0 □, Revitalite, 0.5 h,

RT, over night.

Scheme 3[a]

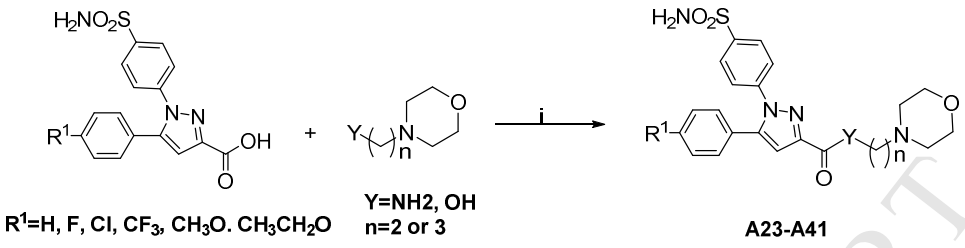

[a] Reagents and conditions: (i) EDC·HCl, HOBt, DMAP, dichloromethane, 0 □, Revitalite, 0.5 h, RT, over night.

Table 1. Structure of target compounds **A1-A22**

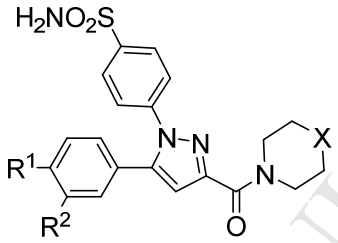

Compds	R^1	R^2	X
A1	H	F	S
A2	H	F	O
A3	H	Cl	S
A4	H	Cl	O
A5	Cl	H	S
A6	Cl	H	O
A7	CH_3CH_2O	H	S
A8	CH_3CH_2O	H	O
A9	F	H	S
A10	F	H	O
A11	CH_3	H	O
A12	CH_3	H	S
A13	Br	H	S
A14	Br	H	O
A15	H	CH_3O	S
A16	H	CH_3O	O
A17	CH_3O	H	S
A18	CH_3O	H	O
A19	CF_3	H	S
A20	CF_3	H	O
A21	H	H	S
A22	H	H	O

Table 2. Structure of target compounds **A23-A41**

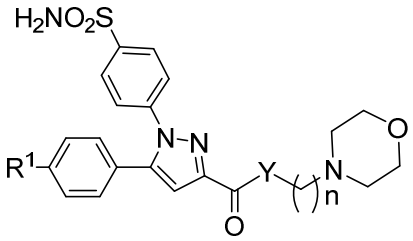

Compds	R^1	Y	n
A23	H	NH	3
A24	H	O	3
A25	H	NH	2
A26	Cl	O	3
A27	Cl	O	2
A28	Cl	NH	2
A29	F	O	2
A30	F	NH	2
A31	F	O	3
A32	CF_3	O	2
A33	CF_3	NH	3
A34	CF_3	O	3
A35	CH_3O	NH	2
A36	CH_3O	O	3
A37	CH_3O	NH	3
A38	CH_3CH_2O	NH	2
A39	CH_3CH_2O	O	3
A40	CH_3CH_2O	NH	3
A41	CH_3CH_2O	O	2

Furthermore, the crystal structure of **A8** (CCDC: 1845660) was determined by X-ray diffraction analysis. The crystal data showed in **Figure 2** and **Table 3**. The data is provided free of charge by The Cambridge Crystallographic Data Center.

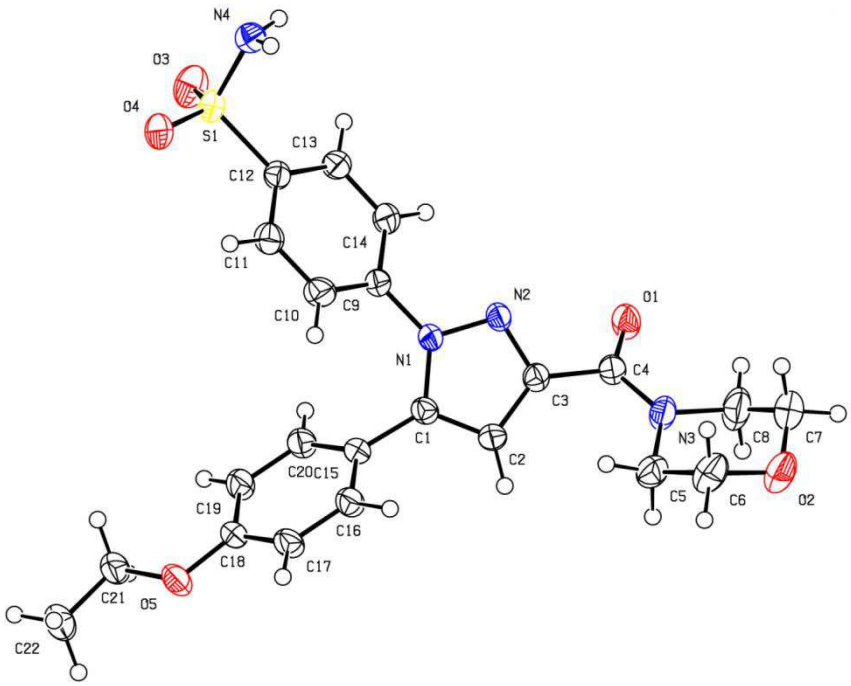

Fig 2. Crystal structure diagram of compound **A8**.

Table 3. Crystal data for compound **A8**

Compounds	**A8**
CCDC number	1845660
Empirical formula	$C_{22}H_{24}N_4O_5S$
Formula weight	456.51
Crystal system	Monoclinic
Space group	$P\ 2_1/c$
a (Å)	7.8754(7)
b (Å)	16.3675(13)
c (Å)	16.9128(14)
β (°)	93.7768(16)
V (Å^3)	2175.3(3)
Z	4
D_c (g cm^{-3})	1.394
μ (mm^{-1})	0.191
F (000)	960.0
θ (°)	2.489-27.523
Reflections collected/unique	4270/3444
R_1, wR_2 [I >2σ(I)]	0.0378, 0.0930
R_1, wR_2 [all data]	0.0501, 0.0982
Goodness-of-fit on F^2	1.052

2.2. MTT assay

All synthesized compounds **A1-A41** were evaluated for *in vitro* antiproliferative activity on five cell lines (F10: murine melanoma, Hela: human cervical cancer, A549: human lung cancer, MCF-7: human breast cancer, 293T: human renal epithelium.) by using MTT assay. **Celecoxib** and an intermediate product **4c** (**Figure 3**) served as positive control. As shown in **Table 4**, most target compounds could effectively inhibit the proliferation of the four test cancer cell lines compared with **Celecoxib** and exhibited lower cytotoxic effects according to the safety trial on 293T cell lines**.** Among them, compounds **A19** and **A33** showed superior growth inhibitory effects to that of **Celecoxib** (IC_{50}: 8.16-10.21 μM of **A19**, 6.43-10.97 μM of **A33** *vs.* 11.04-15.68 μM of **Celecoxib**), and it was worth noting that both compounds have CF_3 group substitution in the para-position of phenyl ring (R^1). Meanwhile, the intermediate **4c** has an IC50 value ranging from 23.79 to 26.51 μM, it was apparent that the introduction of morpholine derivatives significantly enhances the anti-proliferative activity. Compounds **A1** and **A3** showed equivalent anti-proliferative activity to **celecoxib**, but were much less toxic to non-cancer cell line than **celecoxib**, which also indicated that the introduction of morpholine derivatives also plays a positive role in reducing the toxicity of normal cells(*e.g.* F10: 10.35 μM of **A1** *vs.* 13.27 μM of **Celecoxib**; 293T:176.15 μM of **A1** *vs.* 97.87 μM of **Celecoxib**). Interestingly, it was found that these hybrid compounds (**A1, A3, A19, A33**) were linked by the amide linkage. Therefore, it can be assumed that the hydrophobicity of hybrid compounds also contributes to the improvement of

189 antiproliferative activity.

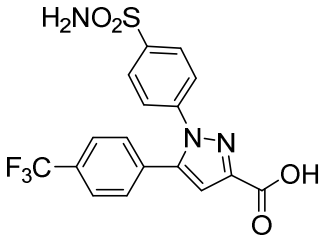

190

191 **Fig. 3.** Structure of **4**

192 **Table 4.** Antiproliferative activities of target compounds, **celecoxib**, and **4c** against different
193 cancer cell lines, and cytotoxicity towards non-cancer cells.

	Cell lines (IC_{50},[a,b] μM ± SD）				
Compds	**F10**	**Hela**	**A549**	**MCF-7**	**293T**
A1	10.35±0.78	13.23±0.87	14.49±0.59	14.39±1.57	176.15±3.68
A2	30.14±0.36	51.27±1.27	25.71±0.16	18.94±0.16	179.76±1.02
A3	13.94±1.09	14.78±0.57	15.43±0.55	12.54±0.46	191.35±1.17
A4	14.63±0.84	17.92±1.59	24.57±1.24	15.79±1.31	113.59±2.19
A5	＞100	＞100	＞100	39.79±0.21	231.63±3.15
A6	＞100	＞100	＞100	＞100	＞300
A7	32.26±0.48	21.57±0.83	＞100	16.51±0.83	168.71±0.59
A8	18.64±0.32	27.15±0.91	41.71±2.17	15.01±1.24	115.54±0.82
A9	26.40±0.93	29.17±1.23	18.19±0.91	18.19±0.50	173.71±1.57
A10	20.47±1.51	＞100	27.47±0.68	20.01±2.19	205.91±0.81
A11	21.37±1.22	＞100	22.79±1.13	17.89±1.38	189.67±0.56
A12	15.49±1.28	13.57±1.33	19.91±0.92	18.13±0.12	105.79±0.83
A13	12.14±0.25	15.95±0.81	17.65±1.28	14.56±0.37	197.47±2.57
A14	＞100	22.62±1.05	19.97±0.17	17.91±0.69	160.40±0.97
A15	12.98±0.11	20.3±0.47	15.98±1.33	17.95±1.84	177.38±0.98
A16	29.17±1.42	＞100	＞100	25.98±0.91	134.09±3.15
A17	13.17±0.59	24.10±0.17	17.19±0.54	19.71±0.94	210.71±0.65
A18	20.81±1.50	21.57±1.36	19.59±0.76	16.03±1.23	206.76±0.56
A19	8.16±0.19	9.94±0.25	10.21±1.52	9.25±1.06	135.51±1.29
A20	21.79±1.08	27.65±0.55	25.19±1.03	19.98±0.31	198.79±0.48
A21	＞100	＞100	30.79±0.37	18.87±0.62	163.54±0.90
A22	16.17±0.38	＞100	26.12±0.35	16.49±0.27	184.48±3.87
A23	21.82±0.54	27.42±0.71	20.47±0.93	18.12±1.27	156.15±2.68
A24	22.68±1.89	22.42±0.85	17.69±0.71	17.19±0.51	95.47±0.48
A25	30.79±1.09	21.79±1.07	＞100	39.17±0.95	151.35±1.37
A26	26.79±1.22	21.37±0.43	＞100	22.14±2.49	188.71±0.98
A27	21.98±1.95	25.37±0.14	22.98±0.48	25.79±0.48	121.96±0.59
A28	＞100	19.97±1.26	19.48±0.92	22.97±0.79	111.86±1.51
A29	18.13±1.28	＞100	＞100	19.31±0.85	145.81±1.24

A30	＞100	＞100	＞100	15.79±1.36	112.25±2.39
A31	＞100	＞100	＞100	＞100	＞300
A32	21.50±0.81	24.56±0.62	27.79±1.28	16.69±1.05	147.78±0.98
A33	6.43±0.14	8.08±0.14	10.97±0.57	7.65±0.82	194.01±0.67
A34	14.40±069	29.79±0.77	15.17±0.04	14.71±0.88	179.47±1.18
A35	19.47±0.93	20.41±0.15	17.59±0.42	15.01±1.27	143.79±0.62
A36	13.71±0.34	26.71±1.27	18.19±0.36	19.79±0.69	169.40±0.17
A37	12.98±0.03	＞100	19.17±0.81	16.31±0.48	199.86±1.46
A38	24.17±1.34	20.81±1.57	16.51±0.53	25.79±0.92	155.09±2.19
A39	＞100	＞100	＞100	15.38±0.67	178.71±0.55
A40	12.88±0.22	19.19±0.98	17.83±0.08	15.01±0.33	137.91±2.28
A41	20.17±1.71	29.78±0.11	21.47±1.12	18.79±0.98	115.52±1.79
4c	23.79±0.78	26.51±0.81	22.46±1.21	24.81±1.01	189.57±0.78
Celecoxib	13.27±1.09	15.68±0.89	11.04±1.94	12.57±1.51	97.87±0.48

[a] IC_{50}: Concentration inhibits 50% of cell growth.

[b] Data are shown as the mean ± SD of three independent experiments (n=3)

2.3. *In vitro* COX-2 and 5-LOX inhibitory activities

Both COX-2 and 5-LOX inhibitory activities of target compounds were evaluated *in vitro*, compared with **Celecoxib** and **Zileuton** as the corresponding positive controls. As summarized in **Table 5.1**, most of the target compounds could effectively suppress COX-2 and 5-LOX activities with IC_{50} values varying from 0.17-7.64 μM and 0.68-3.41 μM respectively (**Celecoxib**, IC_{50} = 0.25 μM; **Zileuton**, IC_{50} = 0.83 μM).

Wherein, hybrid compounds substituted with electron withdrawing groups on the benzene ring (R^1, R^2) exhibited better COX-2 inhibitory activity than those substituted with electron donating groups. For example, when R^2 was hydrogen, different R^1 contributed variously to COX-2 inhibitory activity and showed the order as CF_3 > F > Cl > Br > H > CH_3 > CH_3O > CH_3CH_2O (*e.g.* **A19**, IC_{50} = 0.19 μM *vs.* **A7**, IC_{50} = 0.97 μM). Consistently, it was found that the presence of carbon chains could slightly increase the ability of hybrid compounds to inhibit COX-2, comparing compound

A19 (IC_{50} = 0.19 μM) and compound **A33** (IC_{50} = 0.17 μM). For the 5-LOX inhibitory activity, the IC_{50} values of the two groups of hybrid compounds containing carbon chains (**A23-A41**) and without carbon chains (**A1-A22**) were 0.68-1.01 μM and 0.71-3.41 μM, respectively. Therefore, the increase in hydrophobicity might play a positive role in the inhibition of 5-LOX to some extent. In addition, it was noteworthy that the 5-lox inhibitory activity of the hybrid compounds linking with ester linkage (*e.g.* **A39** and **A41**) was slightly better than those linking with amide linkage(*e.g.* **A38** and **A40**).

Furthermore, based on the results of COX-2 and 5-LOX inhibition and antiproliferative test, compounds **A3**, **A19**, **A33**, and **A34** were selected to test the selectivity between COX-1 and COX-2. As shown in **Table 5.2**, these compounds inhibited favorable COX-1/COX-2 selectivity.

Table 5.1. *In vitro* COX-2 and 5-LOX inhibitory activities

Compds	**IC_{50} ± SD (μM)[a]**	
	COX-2	**5-LOX**
A1	0.19±0.09	1.32±0.13
A2	0.23±0.13	2.01±0.15
A3	0.22±0.07	0.87±0.08
A4	0.24±0.02	1.33±0.29
A5	0.23±0.05	2.31±0.34
A6	0.35±0.09	1.79±0.41
A7	0.97±0.18	0.97±0.21
A8	2.99±0.21	0.95±0.22
A9	0.21±0.05	1.27±0.12
A10	0.23±0.07	0.89±0.17
A11	0.93±0.23	1.24±0.12
A12	0.89±0.14	1.57±0.31
A13	1.28±0.12	1.21±0.21
A14	0.31±0.17	0.98±0.08
A15	1.95±0.28	1.19±0.23
A16	2.25±0.21	0.96±0.09
A17	1.21±0.26	1.01±0.18

A18	2.01±0.25	0.93±0.16
A19	0.19±0.02	0.71±0.13
A20	0.39±0.04	2.59±0.35
A21	0.67±0.15	3.41±0.19
A22	0.69±0.21	1.19±0.17
A23	0.42±0.19	0.93±0.24
A24	0.56±0.27	0.82±0.19
A25	0.64±0.16	0.96±0.19
A26	5.47±0.25	0.85±0.21
A27	0.25±0.09	0.87±0.19
A28	0.31±0.07	0.89±0.11
A29	0.21±0.07	0.84±0.15
A30	0.16±0.02	1.01±0.23
A31	3.57±0.76	0.75±0.08
A32	0.19±0.04	0.81±0.08
A33	0.17±0.07	0.68±0.17
A34	0.21±0.08	0.75±0.12
A35	0.87±0.09	0.91±0.15
A36	1.05±0.14	0.87±0.23
A37	0.71±0.28	0.98±0.06
A38	0.85±0.29	0.86±0.31
A39	7.64±1.16	0.72±0.09
A40	0.91±0.11	0.84±0.23
A41	1.11±0.15	0.79±0.09
Celecoxib	0.25±0.03	--
Zileuton	--	0.83±0.11

[a] Values are means of four determinations

Table 5.2. *In vitro* COX-1 and COX-2 inhibitory activities of selected compounds

Compds	**IC_{50} ± SD (μM)[a]**		**Selectivity Index(SI)[b]**
	COX-1	**COX-2**	
A3	29.35±0.88	0.21±0.07	139.76
A19	30.79±1.02	0.19±0.02	162.05
A33	32.06±2.79	0.17±0.07	188.58
A34	28.52±2.23	0.21±0.08	135.80
Celecoxib	24.47±0.35	0.25±0.03	97.88

[a] The concentration of test compound required to produce 50% inhibition of COX-1/COX-2 is the mean of four determinations.

[b] selectivity index (COX-1 IC_{50}/COX-2 IC_{50})

2.4. Molecular modeling (docking) studies selectivity index

In order to examine the binding mode and interaction, docking study between compound **A33** which had balanced COX-2/5-LOX inhibitory activities and the COX-2 (PDB: 3LN1) and 5-LOX (PDB: 3V99) enzymes were performed (**Figure 4**). The high-resolution structural information about the COX-2 active site had been reported in detail in the previous research[19]. As illustrated in **Figure 4A**, compound **A33** was well inserted into the active pocket of the COX-2 by three hydrogen bonds and the docking score up to 56.34. The fluoro atom formed a hydrogen bond with Arg-106 (angle NH...F = 110.33°, distance = 2.65 Å), one oxygen atom of the sulfonamide group formed a hydrogen bond with Tyr-371 (angle OH...O = 133.36°, distance = 1.97 Å) and the secondary amine of the amide in linkage offered hydrogen bond to the oxygen atom of Ser-339(angle NH...O = 118.93°, distance = 2.11 Å). Furthermore, *Van der Waals*, carbon-hydrogen bonds, π-sigma bonds, and other weaker interactions also increased the binding affinity of the compound with COX-2. As illustrated in **Figure 4B**, the 3D model shows that the bulge of compound **A33** was inserted into the dent of COX-2 completely.

Similarly, based on the previous study on the crystal structure of human 5-LOX enzyme[37]. The docking study was continued to explore the binding of compound **A33** to 5-LOX. As shown in **Figure 4C**, compound **A33** was well embedded into the active site of 5-LOX by six hydrogen bonds, *Van Der Waals*, Carbon-hydrogen bond, Alkyl, and other weak interaction. Fluorine atom of trifluoromethyl formed an H-bond with Glu 172 (angle NH...F = 128.18°, distance = 2.80 Å). Two oxygen atoms

of sulfonamide formed two H-bonds with Lys 173 (angle NH...O = 144.82°, distance = 2.66 Å) and Asn 554 (angle NH...O = 153.33°, distance = 2.21 Å) respectively. Moreover, the secondary amine in linkage formed an H-bond with Ala 672 (angle O...NH = 151.98°, distance = 2.04 Å) and the carbonyl in linkage formed two H-bonds with Gln 363 (angle NH...O = 116.11°, distance = 2.07 Å) and His 367 (angle NH...O = 96.82°, distance = 2.82 Å). These interactions play important role in improving the stability of the complex and increasing the inhibitory activity of 5-LOX. The model of 3D (**Figure 4D**) showed that compound **A33** was inserted into the activity pocket of 5-LOX nicely. In general, these docking studies showed that the hybrids of morpholine derivatives and pyrazole sulfonamide which acted as COX-2/5-LOX dual inhibitors might be promising potent agents.

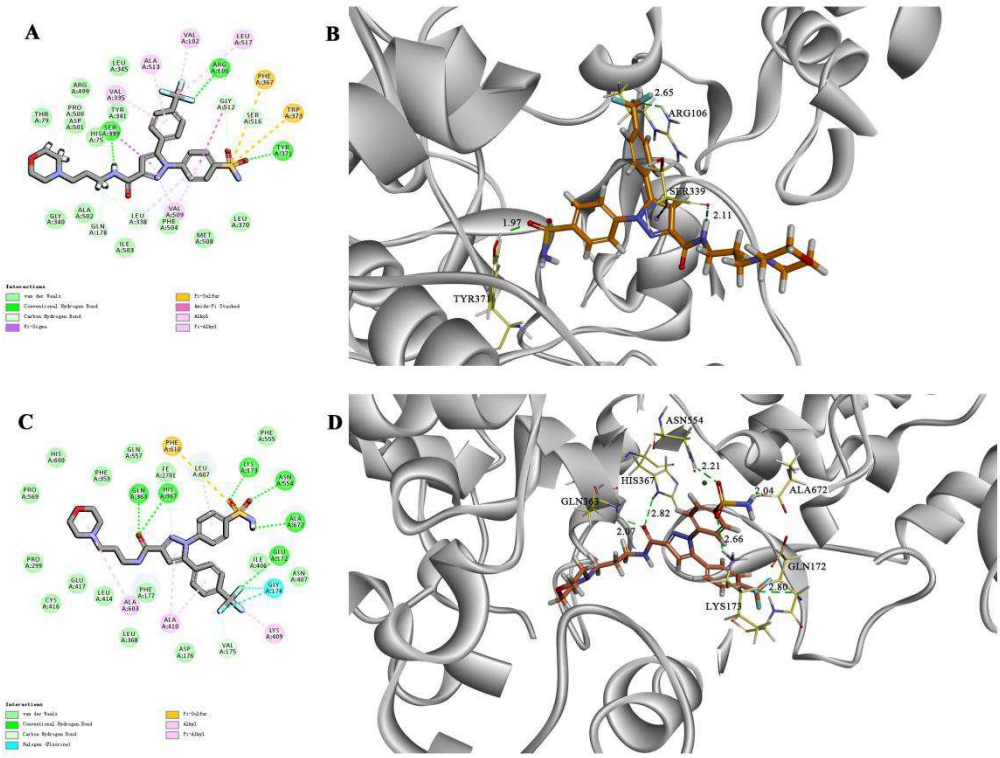

Fig.4. Binding mode of compound **A33** with the COX-2 (PDB code: 3LN1) and 5-LOX (PDB code: 3V99). A) 2D diagram of the interaction between compound **A33** and COX-2; B) 3D models of compound **A33** binding with the active site, only interacting residues are displayed. The hydrogen bond (green) is displayed as dotted arrows. C) 2D diagram of the interaction between compound **A33** and 5-LOX (PDB code: 3V99); D) 3D models of compound **A33** in the 5-LOX pocket. Green lines represent hydrogen bonds.

2.5. Compound A33 induced tumour cell apoptosis

Previous studies had shown that selective COX-2 inhibitors could both inhibit the cell cycle and induce apoptosis of tumor cells, such as **Celecoxib**[38], **Nimesulide**[39]. Therefore, according to the antiproliferative and COX-2/5-LOX inhibitory activity, compound **A33** was selected by using Annexin V/PI double staining assay to detect whether it induced apoptosis of F10 cells. As shown in **Figure 5**, after treatment of F10 cells with compound **A33** at different concentrations (0, 3.125, 6.25, 12.5 and 25 μM) for 48 hours, the apoptotic rate increased significantly from 5.81% to 46.91% and the percentage of apoptosis cells increased in a dose-dependent manner. Subsequently, z-VAD-fmk, a commonly used inhibitor of apoptosis, was used to detect the apoptosis-inducing effect of compound **A33** on F10 cells. The therapeutic concentrations of compound **A33** were the same as above, except that 10 μM of z-VAD-fmk was added while adding various concentrations of compound **A33**. As shown in **Figure 6A**, after treating 10 μM z-VAD-fmk and different concentrations of compound **A33**, the apoptotic rates were 6.96%, 8.83%, 11.08%, 15.91% and 20.4%, respectively. Compared with the addition of the compound **A33** alone, the addition of z-VAD-fmk significantly inhibited the apoptosis of F10 cells caused by the compound **A33** (**Figure 6B**). Taken together, it

could be concluded that compound **A33** could induce F10 cells apoptosis in a dose-dependent manner.

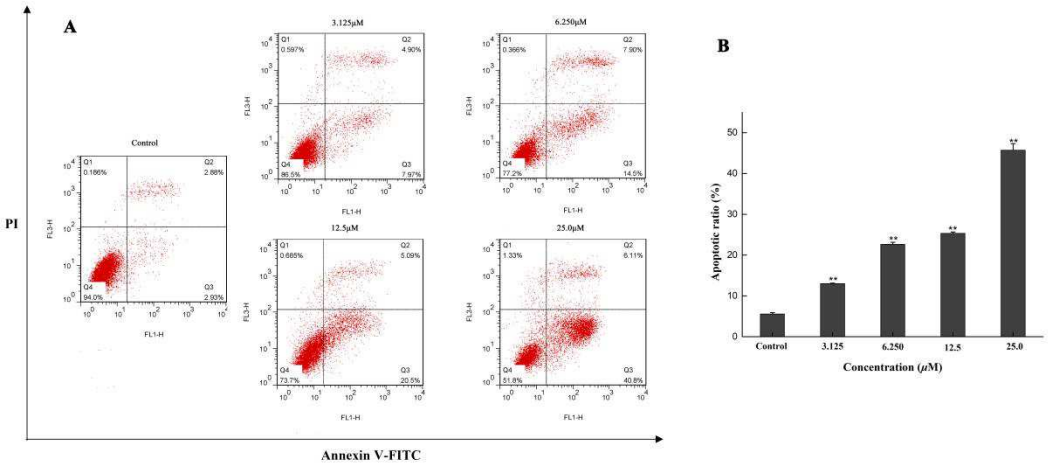

Fig. 5. Compound **A33** induces apoptosis in F10 cell for 48h. A): Flow cytometry analysis of apoptotic F10 cells; B): Apoptotic ratio, Data are shown as mean ± SD of three independent experiments; $^{**}p < 0.01$.

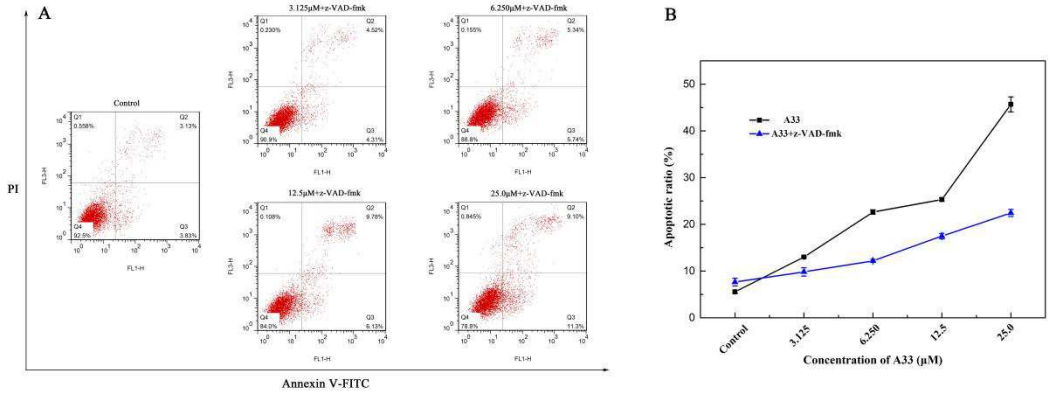

Fig. 6. z-VAD-fmk inhibits apoptosis of F10 cells induced by compound **A33**. A): F10 cell were treated with 0, 3.125, 6.25, 12.5, 25 μM of compound **A33** and z-VAD-fmk (10 μM) for 48h, then apoptotic ratio was analyzed by flow cytometry; B): Comparison of apoptotic ratio between treated with and without z-VAD-fmk. Data are shown as mean ± SD of three independent experiments;

2.6. Compound A33 induced cell cycle arrest

Next, for investigation of the cellular mechanism of anti-proliferation of compound **A33**, further assessment was carried out to check whether compound **A33** could induce the cell cycle arrest of F10 cells by flow cytometry. F10 cells were treated with

different concentrations (0, 3.125, 6.25,12.5, 25 μM) of Compound **A33** for 48 hours. The test results were collected in **Figure 7**. Compared with control group, the percentage of cells in G2 phase was increased from 22.43 to 33.60% with the dose of compound **A33**, while the percentage of cells in G1 phase was decreased from 59.73 to 50.93%. These results indicated that compound **A33** could induce cell cycle arrest in G2 phase with a dose-dependent manner.

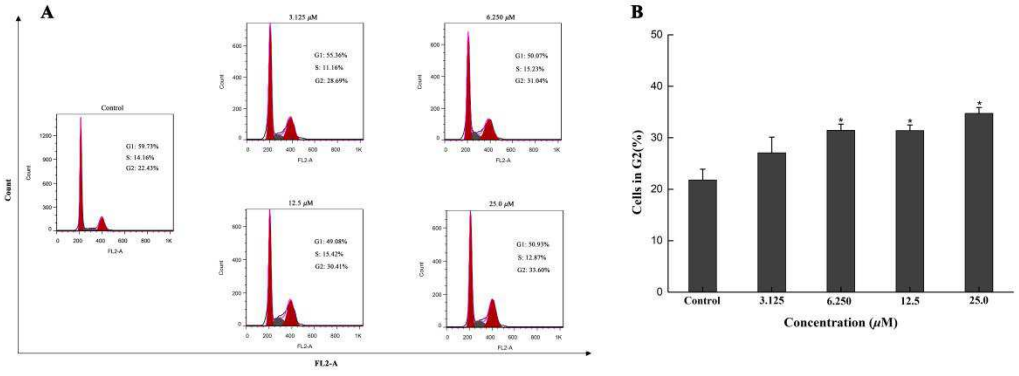

Fig. 7. A). Influence of compound **A33** on F10 cell cycle for 48 h. B). The percentage of cells in G2 graph. Data are shown as mean ± SD of three independent experiments; *p < 0.05.

2.7. Compound A33 inhibited the production of PGE2 in F10 cells

Studies have shown that AA produces prostaglandins under the catalyzed by cyclooxygenase, which is associated with tumor progression. Thus, we tested the ability of compound **A33** to inhibit the production of PGE_2 from AA. After the F10 cells were treated with different doses of lipopolysaccharide (LPS), celecoxib and compound **A33** for 24 hours, the supernatant was collected by centrifugation to detect the expression of PGE_2 with a PGE_2 Enzyme Immunoassay kit. As shown in **Figure 8**, compared with the untreated control group, LPS (1μg/ml) could significantly increase the secretion of PGE_2 in F10 cells, while that was obviously reduced when treated

with celecoxib and compound **A33**. These results indicated that compound **A33** could reduce the production of PGE_2 through COX-2/PGE_2 pathway.

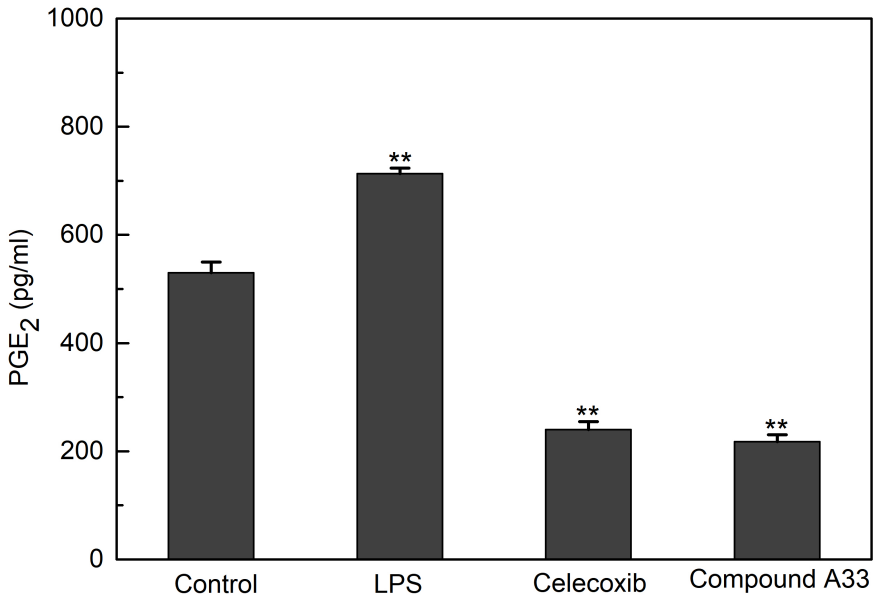

Fig. 8. The effect of LPS (1 μg/ml), Celecoxib (6.25 μM), **A33** (6.25 μM) on PGE_2 secretion in F10 cells. PGE_2 levels were determined by ELISA assay. Data are shown as mean ± SD of three independent experiments; $^{**}p < 0.01$.

2.8. Anti-tumor activity in a xenograft model *in vivo*

Based on the potent anti-proliferative effect and excellent COX-2/5-LOX inhibitory activity of compound **A33** *in vitro*, its antitumor activity was further tested *in vivo*. F10 cells (5×10^6) were injected subcutaneously into the right flank of nude mice to establish xenograft model. When the tumor mass was visible and the tumor size was approximately 100 mm^3, twenty-four tumor-bearing mice were randomly divided into four groups: vehicle, **celecoxib** (20 mg/kg), compound **A33** (20 mg/kg) and compound **A33** (40 mg/kg), administered intraperitoneally once every two days. Mice tumor volume was recorded every other day and the whole treatment period lasted for

two weeks. As shown in **Figure 9A**, the tumor volume in the vehicle group increased rapidly, while the treated groups showed a significant inhibitory effect on the tumor volume. Among them, compound **A33** (20 mg/kg) treated groups did not significantly differ from celecoxib (20 mg/kg) treated group, after 14 days of treatment, the final tumor volumes for these two groups were 1076.58 and 978.35 mm^3, respectively. After the last treatment, the tumors were removed and weighed (**Figure 9B and 9D)**. Compared with the average tumor weight of the vehicle group of 1.24g, other three treated groups showed a marked decrease, wherein compound **A33** (40mg/kg) showed the lightest tumor weight (0.48 ± 0.06 g). Meanwhile, no obvious change was observed in the body weight of treated groups, indicating that the compound **A33** was not toxic for these mice. Conversely, the body weight of the vehicle group increased slightly in the later stage of the treatment period (**Figure 9C)**. Taken together, these data indicated that compound **A33** has excellent anti-tumor activity *in vivo* and is worthy of further study as a promising compound for the development of COX-2/5-LOX dual inhibitors for cancer therapy.

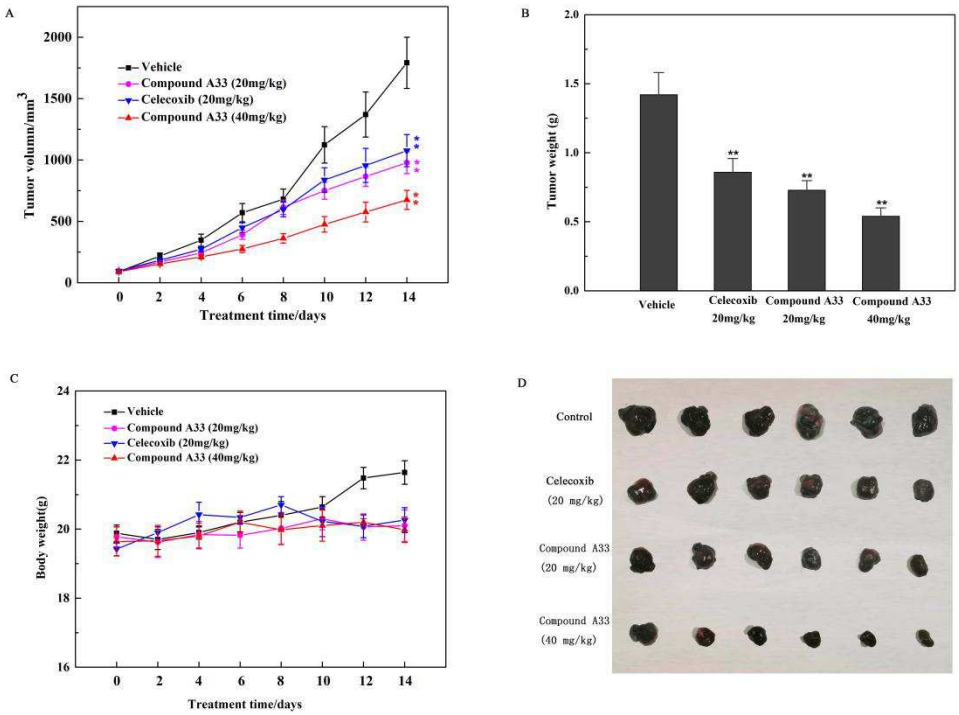

Fig. 9. Compound **A33** effectively inhibited tumor growth in xenografts *in vivo*.(A) Tumour volumes, Data were measured every other day by using a Vernier caliper and calculated as 0.5 × length × width^2 (mm^3). (B) Weight of the excised tumors from each group; (C) body weights of mice from each group. (D) Photograph of the excised tumors from each group after treatment. **p < 0.01.

2.9. Compound A33 pharmacokinetics in tumor-bearing nude mice

We further studied the metabolic stability of compound **A33** after administration in mice. After 24 h of intraperitoneal injection, blood sampling in mice eyes, obtained plasma after centrifugation. The plasma was extracted with ethyl acetate. Then treated sample and compound **A33** were detected by HPLC. As shown in **Figure 10A**, the peak time of Compound **A33** was 39.654 min, injected it into mice for 24 hours. Compound **A33** was detected at 39.950 min (**Figure 10B**). The results showed that compound **A33** was stable *in vivo*, and the amide linkage was not easily cleaved.

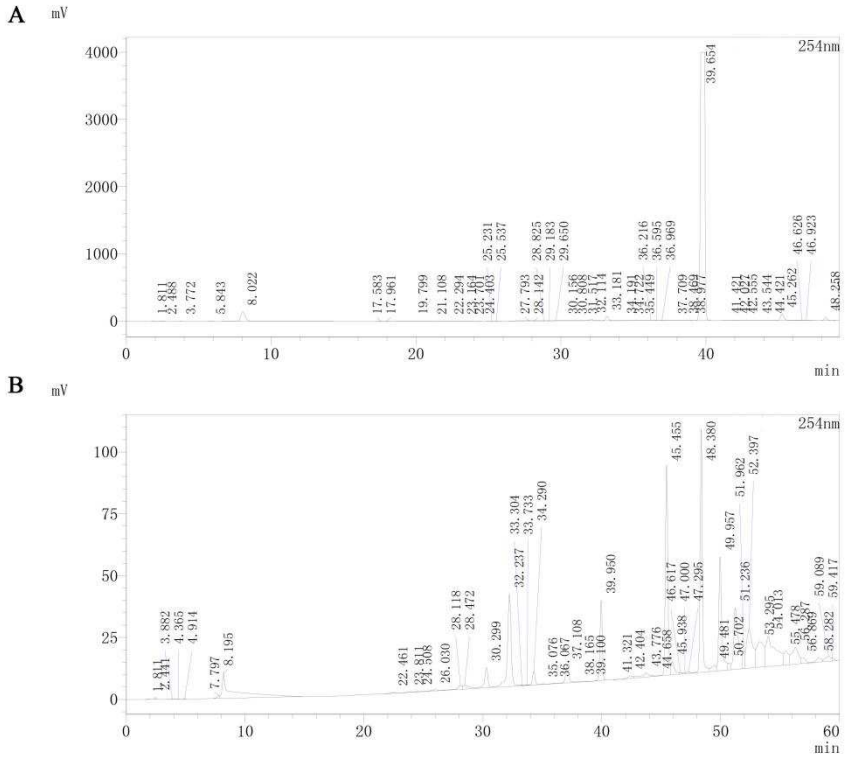

Fig. 10. The image of the test samples by HPLC. (A) Compound **A33**. (B) Extracted from plasma with ethyl acetate.

3. Conclusions

In order to further search for COX-2/5-LOX dual inhibitors that increase cancer treatment while reducing side effects, a series of novel hybrids of diaryl-1,5-diazoles and morpholine derivatives was designed as COX-2/5-LOX dual inhibitors for cancer treatment. Most of the hybrid compounds showed potent inhibitory activity, among which the compound **A33** with CF_3 substituted on the benzene ring (R^1) displayed the most potent activity, and its IC_{50} values against F10, HeLa, A549, MCF-7 cells were 6.43, 8.08, 10.97, 7.65 μM, respectively. At the same time, anti-proliferation and *in vitro* COX-2/5-LOX inhibition experiments showed that the introduction of morpholine derivatives contributed significantly to the reduction of cytotoxicity and the increase of antiproliferative activity. Especially, the representative compound **A33**

exhibited excellent ability to inhibit 5-LOX with the IC_{50} value of 0.68 μM. Further molecular docking studies revealed several interactions between compound **A33** and the active sites of COX-2 and 5-LOX, which might be beneficial for its antiproliferative effects. In mechanistic studies, compound **A33** was observed to induce apoptosis of F10 cells and G2 phase cell arrest in a dose-dependent manner. Furthermore, the *in vivo* anti-tumor activity of compound **A33** was confirmed on F10-xenograft mouse model and pharmacokinetic studies had also demonstrated its satisfying stability *in vivo*. In conclusion, compound **A33** can further be optimized to find innovative anti-tumor drug candidates as COX-2/5-LOX dual inhibitors.

4. Experimental section

4.1. Materials and measurements

All commercial reagents and solvents, purchased from Aladdin (China) and Xiya Reagent, were used in analytical grade. Melting points of all the compounds were determined with an X4 MP apparatus (Jingsong Corp, Shanghai, China). The ^{1}H spectra were both recorded in DMSO-d_6 and $CDCl_3$ using Bruker (Rhenistetten-Forchheim, Germany) AM 600 MHz and Bruker AM 400 MHz, using TMS as an internal standard. ^{1}H NMR and ^{13}C NMR chemical shifts are reported in δ/ppm and coupling constants in Hz. Thin layer chromatography (TLC) plates coated with Merck silica gel 60 GF254 monitored the chemical reactions and the purifying of the products whose spots were visualized under 254/365 nm light. *In vitro* biological evaluation of the synthesized compounds was conducted at State Key Laboratory of Pharmaceutical Biotechnology, Nanjing University, Nanjing.

The COX-1 (human) Inhibitor Screening Assay Kit (catalog No.70117), COX-2 (human) Inhibitor Screening Assay Kit (catalog No.701180), 5-LOX Inhibitor Screening Assay Kit (catalog No.520111) and PGE_2 enzyme immunoassay (EIA) kit-monoclonal (catalog No.514010) were purchased from Cayman Chemical (MI, USA). 3-(4,5-Dimethylthiazol-2-yl)-2,5-diphenyltetrazolium (MTT) were purchased from Beyotime Institute of Biotechnology (Haimen, China). Annexin V-FITC cell apoptosis assay kit (catalog No.BA11100) was purchased from BIO-BOX (Nanjing, China). Caspase Inhibitor Z-VAD-FMK was purchased from Beyotime (Nanjing, China).

4.2. General procedure for the synthesis of compounds 2a-2k

Sodium methoxide (60 mmol) was added slowly to a stirred solution of anhydrous methanol (35 mL) at 0 □, solution of dimethyl oxalate (40 mmol) and the substituted acetophenone (20 mmol) in anhydrous methanol (35 mL) was then gradually added to the mixture with constant stirring, the reaction mixture was then heated at reflux for 6 h. After cooling to room temperature, it was poured into water (200 mL) and acidified with the hydrochloric acid solution (1 mol/L) to PH = 3, then a solid product was immediately formed which was filtered, washed with distilled water. The crude products were purified by recrystallization with ethanol, ethyl acetate and petroleum ether (V_{Etoh}: V_{EtoAc}: V_{PE} = 1: 1: 0.5) washed by ice-water for three times to give pure intermediate products **2a-2k**.

4.3. General procedure for the synthesis of compounds 3a-3k

A mixture of **2a-2k** (10 mmol) and 4-hydrazinylbenzenesulfonamide (10 mmol) in

anhydrous methanol (40 mL) was heated at reflux for 6 h. After cooling to room temperature and pouring it into the water, the precipitate was filtered and washed with ethanol, the solid compounds **3a-3k** were crystallized from ethyl acetate.

4.4. General procedure for the synthesis of compounds 4a-4k

Potassium hydroxide (KOH) (20 mmol) was successively added to a solution of compounds **3a-3k** (4 mmol) in anhydrous methanol, added a few drops of water and the mixture was stirred at 70 □ for 2 hours. After cooling, the mixture solution was poured into water and acidified with the hydrochloric acid solution (1 mol/L) to PH=3, extracted three times with ethyl acetate (3×100 mL) and discarded the aqueous layer. The combined organic extracts were dried with Na_2SO_4, after vacuum evaporation to obtain a solid product **4a-4k**.

4.5. General procedure for the synthesis of compounds A1-A41

To a solution of **4a-4k** (1mmol) in CH_2Cl_2 (20 mL), 1-(3-Dimethylaminopropyl)-3-ethylcarbodiimide hydrochloride (EDC·HCl) (1.2 mmol), 1-Hydroxybenzotriazole (HOBt) (1.2 mmol) and 4-(dimethylamino)pyridine (DMAP) (0.5 mmol) were added in sequence at 0 ˚C. After half an hour of activation, morpholine and substituted morpholine (1.2 mmol) was added and stirred overnight at room temperature. The reaction mixture was washed with the hydrochloric acid solution (1 mol/L, 10 mL), saturated Na_2CO_3 solution (10ml), distilled water (10 mL) three times. The combined organic extracts were dried with Na_2SO_4, The crude product was purified by column chromatography (V_{AcOEt}/V_{PE} = 1/1) to give compounds **A1-A41**.

4-(5-(3-Fluorophenyl)-3-(thiomorpholine-4-carbonyl)-1*H*-pyrazol-1-yl)benzenesu

lfonamide（A1）

White solid, yield 64.1%, m.p. 207.6-208.1 ℃, ^{1}H NMR (400 MHz, DMSO-d_6) δ: 7.87 (d, J = 8.6 Hz, 2H, ArH), 7.55 – 7.46 (m, 6H, ArH), 7.33 (d, J = 8.6 Hz, 2H, -SO_2NH_2), 7.01 (s, 1H, =CH), 4.13 (d, J = 5.6 Hz, 2H, -CH_2), 3.92 (t, J = 4.9 Hz, 2H, -CH_2), 2.70 (t, J = 4.2 Hz, 4H, -CH_2). MS(ESI): 447.52 $[M + H]^+$. Anal. Calcd for $C_{20}H_{19}FN_4O_3S_2$: C, 53.80; H, 4.25; N, 12.55%; Found: C, 54.01; H, 4.24; N, 12.49.

4-(5-(3-Fluorophenyl)-3-(morpholine-4-carbonyl)-1*H*-pyrazol-1-yl)benzenesulfonamide(A2)

White solid, yield 71.6%, m.p. 177.2-177.9 ℃. ^{1}H NMR (600 MHz, DMSO-d_6) δ: 7.89 – 7.85 (m, 2H, ArH), 7.53 (d, J = 8.7 Hz, 2H, ArH), 7.51 – 7.47 (m, 4H, ArH), 7.33 (d, J = 8.6 Hz, 2H, -SO_2NH_2), 7.03 (s, 1H, =CH), 3.97 (t, J = 4.8 Hz, 2H, -CH_2), 3.67 (s, 4H, -CH_2), 3.63 (t, J = 4.8 Hz, 2H, -CH_2). ^{13}C NMR (151 MHz, DMSO-d_6) δ 161.75, 148.04, 143.95, 142.94, 141.78, 134.34, 131.05, 129.38, 128.28, 127.32, 127.30, 126.18, 126.16, 111.05, 67.00, 66.63, 47.69, 42.84. MS(ESI): 431.45 $[M + H]^+$. Anal. Calcd for $C_{20}H_{19}FN_4O_4S$: C, 53.81; H, 4.45; N, 13.02%; Found: C, 53.59; H, 4.43; N, 13.07.

4-(5-(3-Chlorophenyl)-3-(thiomorpholine-4-carbonyl)-1*H*-pyrazol-1-yl)benzenesulfonamide(A3)

White solid, yield 17%, m.p. 22.1-224.8 ℃. ^{1}H NMR (600 MHz, DMSO-d_6) δ: 7.88 (d, J = 6.9 Hz, 2H, ArH), 7.62 (d, J = 6.6 Hz, 2H, ArH), 7.54 (d, J = 8.4 Hz, 2H, ArH), 7.51 (s, 2H, -SO_2NH_2), 7.34 (d, J = 8.6 Hz, 1H, ArH), 7.22 (d, J = 6.9 Hz, 1H, ArH), 7.06 (s, 1H, =CH), 4.12 (t, J = 5.0 Hz, 2H, -CH_2), 3.92 (t, J = 5.0 Hz, 2H, -CH_2), 2.70 (q, J = 5.2 Hz, 4H, -CH_2). MS(ESI): 463.97 $[M + H]^+$. Anal. Calcd for $C_{20}H_{19}ClN_4O_3S_2$: C, 51.89; H, 4.14; N, 12.10%; Found: C, 51.69; H, 4.15; N, 12.05.

4-(5-(3-Chlorophenyl)-3-(morpholine-4-carbonyl)-1*H*-pyrazol-1-yl)benzenesulfonamide(A4)

Light yellow solid, yield 87.2%, m.p. 201.0-201.5 ℃. ^{1}H NMR (DMSO-d_6, 600

MHz); δ: 7.87(d, J= 8.7 Hz, 2H, ArH), 7.63(d, J =1.02 Hz, 2H, ArH), 7.54(d, J =1.92 Hz, 2H, ArH), 7.51(s, 2H, -SO_2NH_2), 7.34(t, J =8.04 Hz, 1H, ArH), 7.21(d, J =7.26 Hz, 1H, ArH), 7.07(s, 1H, =CH), 3.96(t, J =4.26 Hz, 2H, -CH_2-), 3.67(s, 4H, -CH_2-),3.63(t, J =4.26 Hz, 2H, -CH_2). MS(ESI): 447.91 $[M + H]^+$. Anal. Calcd for $C_{20}H_{19}ClN_4O_4S$: C, 53.75; H, 4.29; N, 12.54%; Found: C, 53.54; H, 4.27; N, 12.53.

4-(5-(4-Chlorophenyl)-3-(thiomorpholine-4-carbonyl)-1*H*-pyrazol-1-yl)benzenesulfonamide(A5)

Light yellow solid, yield 27.8%, m.p. 209.6-211.0 □. ^{1}H NMR (600 MHz, DMSO-d_6) δ: 7.87 (d, J = 8.7 Hz, 2H, ArH), 7.54 (d, J = 8.6 Hz, 2H, ArH), 7.50 (s, 2H, -SO_2NH_2), 7.45 (m, 1H, ArH), 7.24 (m, 2H, ArH), 7.09 (d, J = 7.8 Hz, 1H, ArH), 7.05 (s, 1H, =CH), 4.13 (d, J = 6.1 Hz, 2H, -CH_2), 3.93 (d, J = 6.0 Hz, 2H, -CH_2), 2.70 (d, J = 5.1 Hz, 4H, -CH_2). ^{13}C NMR (151 MHz, DMSO-d_6) δ 163.19, 162.05, 148.14, 143.97, 142.81, 141.76, 131.54, 131.42, 131.36, 127.26, 126.13, 125.49, 116.49, 116.29, 116.14, 111.06, 49.82, 44.99, 40.51, 28.04, 27.17. MS(ESI): 463.97 $[M + H]^+$. Anal. Calcd for $C_{20}H_{19}ClN_4O_3S_2$: C, 51.89; H, 4.14; N, 12.10%; Found: C, 51.68; H, 4.15; N, 12.11.

4-(5-(4-Chlorophenyl)-3-(morpholine-4-carbonyl)-1*H*-pyrazol-1-yl)benzenesulfonamide(A6)

White solid, yield 62%, m.p. 179.3-179.6 □, ^{1}H NMR (400 MHz, DMSO-d_6) δ: 7.87 (d, J = 8.5 Hz, 2H, ArH), 7.55 – 7.47 (m, 6H, ArH), 7.33 (d, J = 8.4 Hz, 2H, -SO_2NH_2), 7.02 (s, 1H, =CH), 3.98 (t, J = 4.7 Hz, 2H, -CH_2), 3.65 (d, J = 17.6 Hz, 6H, -CH_2). ^{13}C NMR (151 MHz, DMSO-d_6) δ 161.74, 147.99, 144.03, 142.50, 141.72, 131.85, 131.76, 131.66, 131.26, 128.29, 127.30, 127.22, 126.25, 126.18, 122.45, 111.29, 66.99, 66.63, 47.68, 42.83, 40.56, 40.48, 40.34, 40.06, 39.62. MS(ESI): 447.91 $[M + H]^+$. Anal. Calcd for $C_{20}H_{19}ClN_4O_4S$: C, 53.75; H, 4.29; N, 12.54%; Found: C, 53.54; H, 4.27; N, 12.49.

4-(5-(4-Ethoxyphenyl)-3-(thiomorpholine-4-carbonyl)-1*H*-pyrazol-1-yl)benzenesulfonamide(A7)

White solid, yield 58%, m.p. 229.8-230.6 □, ^{1}H NMR (600 MHz, DMSO-d_6) δ: 7.85 (d, J = 8.6 Hz, 2H, ArH), 7.52 – 7.48 (m, 4H, ArH), 7.21 (d, J = 8.7 Hz, 2H, ArH), 6.95 (d, J = 8.8 Hz, 2H, -SO_2NH_2), 6.88 (s, 1H, =CH), 4.13 (t, J = 5.0 Hz, 2H, -CH_2), 4.04 (q, J = 7.0 Hz, 2H,-OCH_2CH_3), 3.91 (t, J = 5.1 Hz, 2H, -CH_2), 2.69 (q, J = 5.2 Hz, 4H, -CH_2), 1.32 (t, J = 6.9 Hz, 3H,-OCH_2CH_3). MS(ESI): 473.58 $[M + H]^+$. Anal. Calcd for $C_{22}H_{24}N_4O_4S_2$: C, 55.92; H, 5.12; N, 11.86%; Found: C, 55.70; H, 5.13; N, 11.83.

4-(5-(4-Ethoxyphenyl)-3-(morpholine-4-carbonyl)-1*H*-pyrazol-1-yl)benzenesulfonamide(A8)

White solid, yield 29%, m.p. 203.9-204.4□. ^{1}H NMR (600 MHz, DMSO-d_6) δ: 7.86 (d, *J* = 8.6 Hz, 2H, ArH), 7.51 (d, *J* = 8.6 Hz, 2H, ArH), 7.49 (s, 2H, -SO_2NH_2), 7.21 (d, *J* = 8.7 Hz, 2H, ArH), 6.95 (d, *J* = 8.8 Hz, 2H, ArH), 6.90 (s, 1H, =CH), 4.04 (d, *J* = 7.1, 3.6 Hz, 2H,-OCH_2), 3.98 (t, *J* = 4.8 Hz, 2H, -CH_2), 3.67 (s, 4H, -CH_2), 3.63 (t, *J* = 4.8 Hz, 2H, -CH_2), 1.32 (t, *J* = 7.0 Hz, 3H, -CH_3). MS(ESI): 457.52 $[M + H]^+$. Anal. Calcd for $C_{22}H_{24}N_4O_5S$: C, 57.88; H, 5.30; N, 12.27%; Found: C, 57.82; H, 5.28; N, 12.23.

4-(5-(4-Fluorophenyl)-3-(thiomorpholine-4-carbonyl)-1*H*-pyrazol-1-yl)benzenesulfonamide(A9)

White solid, yield 27.8%, m.p. 115.4-116.7 □. ^{1}H NMR (600 MHz, DMSO-d_6) δ: 7.86 (d, *J* = 8.7 Hz, 2H, ArH), 7.51 (d, *J* = 8.7 Hz, 2H, ArH), 7.49 (s, 2H, -SO_2NH_2), 7.37 (m, 2H, ArH), 7.28 (t, *J* =8.8 Hz, 2H, ArH), 6.98 (s, 1H, =CH), 4.14 (s, 2H, -CH_2), 3.92 (s, 2H, -CH_2), 2.70 (d, *J* = 4.9 Hz, 4H, -CH_2). ^{13}C NMR (151 MHz, DMSO-d_6) δ 162.12, 148.10, 143.18, 141.84, 131.64, 131.58, 127.26, 126.04, 116.45, 116.31, 110.69, 49.81, 44.98, 40.52, 28.05, 27.17. MS(ESI): 447.52 $[M + H]^+$. Anal. Calcd for $C_{20}H_{19}FN_4O_3S_2$: C, 53.80; H, 4.29; N, 12.55%; Found: C, 53.60; H, 4.30; N, 12.56.

4-(5-(4-Fluorophenyl)-3-(morpholine-4-carbonyl)-1*H*-pyrazol-1-yl)benzenesulfonamide(A10)

White solid, yield 17.1%, m.p. 241.3-242.6 □. ^{1}H NMR (600 MHz, DMSO-d_6) δ: 7.86 (d, J = 8.6 Hz, 2H, ArH), 7.51 (d, J = 8.6 Hz, 2H, ArH), 7.49 (s, 2H, -SO_2NH_2), 7.37 (m, 2H, ArH), 7.28 (t, J = 8.8 Hz, 2H, ArH), 6.99 (s, 1H, =CH), 3.98 (t, J = 4.8 Hz, 2H, -CH_2), 3.67 (s, 4H, -CH_2), 3.63 (t, J = 4.8 Hz, 2H, -CH_2). MS(ESI): 431.45 $[M + H]^+$. Anal. Calcd for $C_{20}H_{19}FN_4O_4S$: C, 55.81; H, 4.45; N, 13.02%; Found: C, 55.59; H, 4.43; N, 13.05.

4-(3-(Morpholine-4-carbonyl)-5-(p-tolyl)-1*H*-pyrazol-1-yl)benzenesulfonamide(A11)

White solid, yield 68.8%, m.p. 206.3-206.6 □. ^{1}H NMR (600 MHz, DMSO-d_6) δ: 7.85 (d, J = 8.6 Hz, 2H, ArH), 7.51 (d, J = 8.7 Hz, 2H, ArH), 7.49 (s, 2H, -SO_2NH_2), 7.22 (d, J = 8.0 Hz, 2H, ArH), 7.19 (d, J = 8.2 Hz, 2H, ArH), 6.94 (s, 1H, =CH), 3.98 (t, J = 4.8 Hz, 2H, -CH_2), 3.67 (s, 4H, -CH_2), 3.63 (t, J = 4.8 Hz, 2H, -CH_2), 2.32 (s, 3H, -CH_3). ^{13}C NMR (151 MHz, DMSO-d_6) δ 161.89, 147.96, 144.19, 143.78, 142.08, 139.12, 129.88, 129.08, 127.21, 126.50, 126.12, 110.48, 67.00, 66.64, 47.68, 42.83, 40.49, 21.27. MS(ESI): 427.49 $[M + H]^+$. Anal. Calcd for $C_{21}H_{22}N_4O_4S$: C, 59.14; H, 5.20; N, 13.14%; Found: C, 59.21; H, 5.21; N, 13.15.

4-(3-(Thiomorpholine-4-carbonyl)-5-(p-tolyl)-1*H*-pyrazol-1-yl)benzenesulfonamide(A12)

White solid, yield 66.6%, m.p. 185.5-186.2 □. ^{1}H NMR (600 MHz, DMSO-d_6) δ: 7.85 (d, J = 8.7 Hz, 2H, ArH), 7.51 (d, J = 8.7 Hz, 2H, ArH), 7.49 (s, 2H, -SO_2NH_2), 7.22 (d, J = 8.0 Hz, 2H, ArH), 7.19 (d, J = 8.2 Hz, 2H, ArH), 6.92 (s, 1H, =CH), 4.14 (d, J = 7.4 Hz, 2H, -CH_2), 3.91 (d, J = 6.0 Hz, 2H, -CH_2), 2.69 (d, J = 5.5 Hz, 4H, -CH_2).2.32 (s,3H, -CH_3). ^{13}C NMR (151 MHz, DMSO-d_6) δ 162.19, 148.12, 143.74, 142.07, 129.89, 129.08, 127.21, 126.52, 126.02, 110.31, 49.81, 44.98, 40.52, 28.04, 27.17, 21.28. MS(ESI): 443.55 $[M + H]^+$. Anal. Calcd for $C_{21}H_{22}N_4O_3S_2$: C, 56.99; H, 5.01; N, 12.66%; Found: C, 56.76; H, 5.02; N, 12.61.

4-(5-(4-Bromophenyl)-3-(thiomorpholine-4-carbonyl)-1*H*-pyrazol-1-yl)benzenesulfonamide(A13)

White solid, yield 63.5%, m.p. 184.1-185.2 □, ^{1}H NMR (400 MHz, DMSO-d_6) δ: 7.87 (d, J = 8.6 Hz, 2H, ArH), 7.63 (d, J = 8.5 Hz, 2H, ArH), 7.55 – 7.48 (m, 4H, ArH), 7.26 (d, J = 8.5 Hz, 2H, -SO_2NH_2), 7.01 (s, 1H, =CH), 4.13 (s, 2H, -CH_2), 3.91 (d, J = 6.0 Hz, 2H, -CH_2), 2.69 (d, J = 5.6 Hz, 4H, -CH_2). MS(ESI): 508.42 $[M + H]^+$. Anal. Calcd for $C_{20}H_{19}BrN_4O_3S_2$: C, 47.34; H, 3.77; N, 11.04%; Found: C, 47.51; H, 3.75; N, 11.07.

4-(5-(4-Bromophenyl)-3-(morpholine-4-carbonyl)-1*H*-pyrazol-1-yl)benzenesulfonamide(A14)

White solid, yield 19%, m.p. 151.6-153.2 □. ^{1}H NMR (600 MHz, DMSO-d_6) δ: 7.87 (d, J = 8.6 Hz, 2H, ArH), 7.63 (d, J = 8.5 Hz, 2H, ArH), 7.53 (d, J = 8.6 Hz, 2H, ArH), 7.49 (s, 2H, -SO_2NH_2), 7.26 (d, J = 8.5 Hz, 2H, ArH), 7.03 (s, 1H, =CH), 3.97 (t, J = 4.9 Hz, 2H, -CH_2), 3.67 (s, 4H, -CH_2), 3.63 (t, J = 4.8 Hz, 2H, -CH_2). MS(ESI): 492.36 $[M + H]^+$. Anal. Calcd for $C_{20}H_{19}BrN_4O_4S$: C, 48.89; H, 3.90; N, 11.40%; Found: C, 48.71; H, 3.91; N, 11.43.

4-(5-(3-Methoxyphenyl)-3-(thiomorpholine-4-carbonyl)-1*H*-pyrazol-1-yl)benzenesulfonamide(A15)

Light yellow solid, yield 51.6%, m.p. 196.8-197.3 □. ^{1}H NMR (600 MHz, DMSO-d_6) δ: 7.86 (d, J = 8.5 Hz, 2H, ArH), 7.53 (d, J = 8.5 Hz, 2H, ArH), 7.50 (s, 2H, -SO_2NH_2), 7.31 (t, J = 8.0 Hz, 1H, ArH), 6.99 (m, 2H, ArH), 6.89 (s, 1H, =CH), 6.81 (d, J = 1.9 Hz, 1H, ArH), 4.14 (s, 2H, -CH_2), 3.92 (m, 2H, -CH_2), 3.70 (s, 3H, -CH_3O), 2.70 (q, J = 5.2 Hz, 4H, -CH_2). MS(ESI): 459.55 $[M + H]^+$. Anal. Calcd for $C_{21}H_{22}N_4O_4S_2$: C, 55.01; H, 4.84; N, 12.22%; Found: C, 54.79; H, 4.84; N, 12.17.

4-(5-(3-Methoxyphenyl)-3-(morpholine-4-carbonyl)-1*H*-pyrazol-1-yl)benzenesulfonamide(A16)

Light yellow solid, yield 21%, m.p. 241.3-245.8 □. ^{1}H NMR (400 MHz, DMSO-d_6) δ: 7.87 (d, J = 8.3 Hz, 2H, ArH), 7.53 (d, J = 8.4 Hz, 2H, ArH), 7.50 (s, 2H, -SO_2NH_2), 7.31 (t, J = 7.9 Hz, 1H, ArH), 6.99 (m, 2H, ArH),6.89 (s, 1H, ArH) 6.83 – 6.79 (m, 1H, =CH), 3.98 (t, J = 5.2 Hz, 2H, -CH_2), 3.69 (s, 3H, -CH_3O), 3.67 (s,

4H,-CH_2), 3.63(t, *J* = 6.96 Hz, 2H, -CH_2). ^{13}C NMR (151 MHz, DMSO-d_6) δ 162.07, 148.14, 143.98, 142.52, 141.72, 132.31, 131.80, 131.67, 131.26, 128.30, 127.27, 126.12, 122.45, 111.09, 49.82, 44.99, 40.51, 28.05, 27.18. MS(ESI): 443.49 $[M + H]^+$. Anal. Calcd for $C_{21}H_{22}N_4O_5S$: C, 57.00; H, 5.01; N, 12.66%; Found: C, 56.77; H, 5.02; N, 12.61.

4-(5-(4-Methoxyphenyl)-3-(thiomorpholine-4-carbonyl)-1*H*-pyrazol-1-yl)benzene sulfonamide(A17)

White solid, yield 59.1%, m.p. 222.5-223 □, ^{1}H NMR (400 MHz, DMSO-d_6) δ: 7.86 (d, *J* = 8.3 Hz, 2H, ArH), 7.54 – 7.46 (m, 4H, ArH), 7.23 (d, *J* = 8.3 Hz, 2H, ArH), 6.98 (d, *J* = 8.4 Hz, 2H, -SO_2NH_2), 6.89 (s, 1H, =CH), 4.14 (d, *J* = 5.5 Hz, 2H, -CH_2), 3.91 (d, *J* = 6.0 Hz, 2H, -CH_2), 3.78 (s, 3H, -OCH3), 2.69 (d, *J* = 6.3 Hz, 4H, -CH_2). MS(ESI): 459.55 $[M + H]^+$. Anal. Calcd for $C_{21}H_{22}N_4O_4S_2$: C, 55.01; H, 4.84; N, 12.22%; Found: C, 54.79; H, 4.83; N, 12.18.

5-(5-(4-Methoxyphenyl)-3-(morpholine-4-carbonyl)-1*H*-pyrazol-1-yl) benzene sulfonamide(A18)

White solid, yield 19%, m.p. 203.5-204.0 □. ^{1}H NMR (600 MHz, DMSO-d_6); δ: 7.86(d, *J*= 12.6 Hz, 2H, ArH), 7.51(d, *J* =12.6 Hz, 2H, ArH), 7.49(s, 2H, -SO_2NH_2), 7.23(d, *J* =12.78 Hz, 2H, ArH), 6.97(d, *J* =12.84 Hz, 2H, ArH), 6.90(s, 1H, =CH), 3.98(t, 2H, *J* =8.4, -CH_2-), 3.77(s, 3H, -CH_3O-),3.65 (d, *J* = 16.6 Hz, 6H, -CH_2). ^{13}C NMR (151 MHz, DMSO-d_6) δ 161.91, 160.15, 147.93, 144.03, 143.72, 142.14, 130.61, 127.21, 126.06, 121.58, 114.76, 110.26, 67.01, 66.64, 60.24, 55.72, 47.69, 42.82, 40.51, 14.56. MS(ESI): 443.49 $[M + H]^+$. Anal. Calcd for $C_{21}H_{22}N_4O_5S$: C, 57.00; H, 5.01; N, 12.66%; Found: C, 56.77; H, 5.03; N, 12.67.

4-(3-(Thiomorpholine-4-carbonyl)-5-(4-(trifluoromethyl)phenyl)-1*H*-pyrazol-1-yl)benzenesulfonamide(A19)

Light yellow solid, yield 66.7%, m.p. 197.1-198.8 □. ^{1}H NMR (600 MHz, DMSO-d_6) δ: 7.88 (d, *J* = 8.6 Hz, 2H, ArH), 7.80 (d, *J* = 8.2 Hz, 2H, ArH), 7.55 (m, 4H, ArH), 7.50 (s, 2H, -SO_2NH_2), 7.11 (s, 1H, =CH), 4.14 (t, *J* = 4.9 Hz, 2H, -CH_2),

3.93 (t, *J* = 5.0 Hz, 2H, -CH_2), 2.70 (q, *J* = 5.2 Hz, 4H, -CH_2). ^{13}C NMR (151 MHz, DMSO-d_6) δ 161.99, 148.29, 144.04, 142.66, 141.67, 133.46, 130.05, 129.68, 129.47, 127.38, 126.22, 126.17, 125.33, 111.47, 49.84, 45.01, 40.52, 28.05, 27.17. MS(ESI): 497.52 $[M + H]^+$. Anal. Calcd for $C_{21}H_{19}F_3N_4O_3S_2$: C, 50.80; H, 3.86; N, 11.28%; Found: C, 50.71; H, 3.85; N, 11.24.

4-(3-(Morpholine-4-carbonyl)-5-(4-(trifluoromethyl)phenyl)-1*H*-pyrazol-1-yl)benzenesulfonamide(A20)

White solid, yield 21.4%, m.p. 224.8-225.3 □. ^{1}H NMR (600 MHz, DMSO-d_6) δ: 7.88 (d, *J* = 8.7 Hz, 2H, ArH), 7.80 (d, *J* = 8.5 Hz, 2H, ArH), 7.55 (m, 4H, ArH), 7.50 (s, 2H, -SO_2NH_2), 7.13 (s, 1H, =CH), 3.98 (t, *J* = 4.6 Hz, 2H, -CH_2), 3.68 (s, 4H, -CH_2), 3.63 (d, *J* = 4.5 Hz, 2H, -CH_2). ^{13}C NMR (151 MHz, DMSO-d_6) δ 161.65, 148.13, 144.08, 142.63, 141.66, 133.44, 130.04, 129.67, 129.46, 127.53, 127.37, 126.73, 126.24, 126.20, 126.17, 126.15, 125.32, 123.52, 111.65, 66.99, 66.63, 47.69, 42.84, 40.51. MS(ESI): 481.46 $[M + H]^+$. Anal. Calcd for $C_{21}H_{19}F_3N_4O_4S$: C, 52.50; H, 3.99; N, 11.66%; Found: C, 52.29; H, 3.97; N, 11.70.

4-(5-Phenyl-3-(thiomorpholine-4-carbonyl)-1*H*-pyrazol-1-yl)benzenesulfonamide (A21)

White solid, yield 53.5%, m.p. 192.8-193.9 □. ^{1}H NMR (600 MHz, DMSO-d_6) δ: 7.86 (d, *J* = 8.6 Hz, 2H, ArH), 7.51 (m, 4H, ArH), 7.42 (m, 3H, ArH), 7.31 (m, 2H, -SO_2NH_2), 6.97 (s, 1H, =CH), 4.15 (t, *J* = 4.8 Hz, 2H, -CH_2), 3.92 (t, *J* = 5.0 Hz, 2H, -CH_2), 2.70 (m, 4H, -CH_2). MS(ESI): 429.53 $[M + H]^+$. Anal. Calcd for $C_{20}H_{20}N_4O_3S_2$: C, 56.06; H, 4.70; N, 13.07%; Found: C, 55.84; H, 4.71; N, 13.11.

4-(3-(Morpholine-4-carbonyl)-5-phenyl-1*H*-pyrazol-1-yl)benzenesulfonamide(A22)

Dark yellow solid, yield 87.1%, m.p. 201.0-201.5 □, ^{1}H NMR (600 MHz, DMSO-d_6) δ: 7.86 (d, *J* = 8.6 Hz, 2H, ArH), 7.53 – 7.48 (m, 4H, ArH), 7.43 – 7.40 (m,

3H,ArH), 7.33 – 7.29 (m, 2H,-SO_2NH_2), 6.99 (s, 1H, =CH,), 3.99 (t, *J* = 4.8 Hz, 2H,-CH_2), 3.65 (d, *J* = 25.2 Hz, 6H,-CH_2). MS(ESI): 413.46 $[M + H]^+$. Anal. Calcd for $C_{20}H_{20}N_4O_4S$: C, 58.24; H, 4.89; N, 13.58%; Found: C, 58.43; H, 4.87; N, 13.59.

_N_-(3-Morpholinopropyl)-5-phenyl-1-(4-sulfamoylphenyl)-1*H*-pyrazole-3-carboxamide(A23)

Dark yellow solid, yield 34.7%, m.p. 101.9-102.8 □. ^{1}H NMR (600 MHz, DMSO-d_6) δ: 8.53 (t, *J*= 5.8 Hz, 1H, -CONH), 7.87 (d, *J*= 8.6 Hz, 2H, ArH), 7.57 – 7.48 (m, 4H, ArH), 7.43 – 7.35 (m, 3H, ArH), 7.30 (dd, *J*= 6.7, 2.9 Hz, 2H, -SO_2NH_2), 7.03 (s, 1H, =CH), 3.61 (t, *J*= 4.7 Hz, 4H, -CH_2), 3.34 (q, *J*= 6.5 Hz, 2H, -$CONHCH_2$), 2.47 (m, 6H, -CH2, -$CONHCH_2CH_2CH_2$), 1.73 (p, *J*= 6.9 Hz, 2H, -$CONHCH_2CH_2$). MS(ESI): 470.56 $[M + H]^+$. Anal. Calcd for $C_{23}H_{27}N_5O_4S$: C, 58.83; H, 5.80; N, 14.92%; Found: C, 59.01; H, 5.81; N, 14.93.

3-Morpholinopropyl-5-phenyl-1-(4-sulfamoylphenyl)-1*H*-pyrazole-3-carboxylate (A24)

Light yellow solid, yield 17.3%, m.p. 94.4-95 □. ^{1}H NMR (600 MHz, Chloroform-*d*) δ: 7.85 (d, *J*= 8.3 Hz, 2H, ArH), 7.47 – 7.35 (m, 5H, ArH), 7.28 (s, 2H, -SO_2NH_2), 7.23 – 7.19 (m, 2H, ArH), 7.06 (s, 1H, =CH), 4.51 (t, *J*= 6.1 Hz, 2H, -$COOCH_2$), 3.93 (s, 4H, -CH2), 2.90 (s, 6H, -CH_2, -$COOCH_2CH_2CH_2$), 2.27 (s, 2H, -$COOCH_2CH_2$). MS(ESI): 471.54 $[M + H]^+$. Anal. Calcd for $C_{23}H_{26}N_4O_5S$: C, 58.71; H, 5.57; N, 11.91%; Found: C, 58.93; H, 5.55; N, 11.93.

_N_-(2-morpholinoethyl)-5-phenyl-1-(4-sulfamoylphenyl)-1*H*-pyrazole-3-carboxamide(A25)

Light yellow solid, yield 15.7%, m.p. 95.3-96.1 □. ^{1}H NMR (600 MHz, Chloroform-*d*) δ: 7.91 (d, *J*= 8.3 Hz, 2H, ArH), 7.46 (d, *J*= 8.6 Hz, 2H, ArH), 7.42 – 7.35 (m, 3H, ArH), 7.28 (s, 2H, -SO_2NH_2), 7.22 (d, *J*= 7.1 Hz, 2H, ArH), 7.05 (s, 1H, =CH), 3.88 (s, 4H, -CH_2), 3.74 (s, 2H, -$CONHCH_2$), 2.83 (d, *J*= 52.3 Hz, 6H, -CH_2, -$CONHCH_2CH_2$). MS(ESI): 456.53 $[M + H]^+$. Anal. Calcd for $C_{22}H_{25}N_5O_4S$: C, 58.01; H, 5.53; N, 15.37%; Found: C, 58.21; H, 5.54; N, 15.42.

3-Morpholinopropyl-5-(4-chlorophenyl)-1-(4-sulfamoylphenyl)-1*H*-pyrazole-3-carboxylate(A26)

White solid, yield 58.9%, m.p. 177.2-177.5 □. ^{1}H NMR (600 MHz, Chloroform-*d*) *δ*: 7.78 (d, *J*= 8.6 Hz, 2H, ArH), 7.40 (d, *J*= 8.6 Hz, 2H, ArH), 7.34 (d, *J*= 8.4 Hz, 2H, ArH), 7.13 (d, *J*= 8.5 Hz, 2H, ArH), 7.08 (s, 1H, =CH), 6.42 (s, 2H, $-SO_2NH_2$), 4.55 (s, 2H, $-COOCH_2$), 3.78 (s, 4H, $-CH_2$), 2.87 (s, 2H, $-COOCH_2CH_2CH_2$), 2.63 (s, 4H, $-CH_2$), 1.69 (s, 2H, $-COOCH_2CH_2$). MS(ESI): 505.99 $[M + H]^+$. Anal. Calcd for $C_{23}H_{25}ClN_4O_5S$: C, 54.71; H, 4.99; N, 11.09%; Found: C, 54.81; H, 4.98; N, 11.12.

2-Morpholinoethyl-5-(4-chlorophenyl)-1-(4-sulfamoylphenyl)-1*H*-pyrazole-3-carboxylate(A27)

Light yellow solid, yield 54.5%, m.p. 105.3-106.1 □. ^{1}H NMR (600 MHz, DMSO-d_6) *δ*: 7.92 – 7.85 (m, 2H, ArH), 7.58 – 7.46 (m, 6H, ArH), 7.34 (d, *J*= 8.5 Hz, 2H, $-SO_2NH_2$), 7.21 (s, 1H, =CH), 4.43 (t, *J*= 5.8 Hz, 2H, $-COOCH_2$), 3.57 (t, *J*= 4.7 Hz, 4H, $-CH_2$), 2.69 (t, *J*= 5.8 Hz, 2H, $-COOCH_2CH_2$), 2.49 (s, 4H, $-CH_2$). MS(ESI): 491.96 $[M + H]^+$. Anal. Calcd for $C_{22}H_{23}ClN_4O_5S$: C, 53.82; H, 4.72; N, 11.41%; Found: C, 54.02; H, 4.71; N, 11.44.

5-(4-Chlorophenyl)-*N*-(2-morpholinoethyl)-1-(4-sulfamoylphenyl)-1*H*-pyrazole-3-carboxamide(A28)

Light yellow solid, yield 33.6%, m.p. 106.6-107.3 □. ^{1}H NMR (600 MHz, DMSO-d_6) *δ*: 8.30 (t, *J*= 5.9 Hz, 1H, -CONH), 7.91 – 7.84 (m, 2H, ArH), 7.56 – 7.47 (m, 6H, ArH), 7.35 – 7.29 (m, 2H, $-SO_2NH_2$), 7.07 (s, 1H, =CH), 3.58 (t, *J*= 4.7 Hz, 4H, $-CH_2$), 3.41 (q, *J*= 6.5 Hz, 2H, $-CONHCH_2$), 2.43 (d, *J*= 40.8 Hz, 6H, $-CH_2$, $-CONHCH_2CH_2$). MS(ESI): 490.98 $[M + H]^+$. Anal. Calcd for $C_{22}H_{24}ClN_5O_4S$: C, 53.93; H, 4.94; N, 14.29%; Found: C, 53.72; H, 4.95; N, 14.33.

2-Morpholinoethyl-5-(4-fluorophenyl)-1-(4-sulfamoylphenyl)-1*H*-pyrazole-3-carboxylate(A29)

Light yellow solid, yield 65.3%, m.p. 102.7-103.6□. ^{1}H NMR (600 MHz, Chloroform-*d*) *δ*: 7.83 – 7.77 (m, 2H, ArH), 7.40 – 7.35 (m, 2H, ArH), 7.28 (s, 2H, ArH), 7.20 – 7.14 (m, 2H, -SO_2NH_2), 7.10 – 7.03 (m, 3H, ArH, =CH), 4.61 (t, *J*= 5.4 Hz, 2H, -$COOCH_2$), 3.84 (t, *J*= 4.8 Hz, 4H, -CH_2), 3.02 (d, *J*= 5.3 Hz, 2H, -$COOCH_2CH_2$), 2.84 – 2.75 (m, 4H, -CH_2). MS(ESI): 475.51 $[M + H]^+$. Anal. Calcd for $C_{22}H_{23}FN_4O_5S$: C, 55.69; H, 4.89; N, 11.81%; Found: C, 55.47; H, 4.87; N, 11.84.

5-(4-Fluorophenyl)-*N*-(2-morpholinoethyl)-1-(4-sulfamoylphenyl)-1*H*-pyrazole-3-carboxamide(A30)

Light yellow solid, yield 60.5%, m.p. 99.7-100.1 □. ^{1}H NMR (600 MHz, Chloroform-*d*) *δ*: 7.95 – 7.90 (m, 2H, ArH), 7.51 (s, 1H, ArH), 7.45 – 7.41 (m, 2H, ArH), 7.28 (s, 1H, ArH), 7.23 – 7.18 (m, 2H, ArH), 7.07 (t, *J*= 8.5 Hz, 2H, -SO_2NH_2), 7.03 (s, 1H, =CH), 3.77 (t, *J*= 4.7 Hz, 4H, -CH_2), 3.64 (q, *J*= 5.9 Hz, 2H, -$CONHCH_2$), 2.71 (t, *J*= 6.2 Hz, 2H, -$CONHCH_2CH_2$), 2.62 (s, 4H, -CH_2). MS(ESI): 474.52 $[M + H]^+$. Anal. Calcd for $C_{22}H_{24}FN_5O_4S$: C, 55.80; H, 5.11; N, 14.79%; Found: C, 55.58; H, 5.13; N, 14.82.

3-Morpholinopropyl-5-(4-fluorophenyl)-1-(4-sulfamoylphenyl)-1*H*-pyrazole-3-carboxylate1(A31)

Light yellow solid, yield 39.8%, m.p. 110.2-111.3 □. ^{1}H NMR (600 MHz, Chloroform-*d*) *δ*: 7.89 (d, *J*= 8.7 Hz, 2H, ArH), 7.49 – 7.42 (m, 2H, ArH), 7.28 (s, 2H, -SO_2NH_2), 7.24 – 7.18 (m, 2H, ArH), 7.08 (t, *J*= 8.6 Hz, 2H, ArH), 7.02 (s, 1H, =CH), 4.47 (t, *J*= 6.5 Hz,2H, -$COOCH_2$), 3.75 (t, *J*= 4.7 Hz, 4H, -CH_2), 2.60 – 2.50 (m, 6H, -CH_2, -$COOCOH_2CH_2CH_2$), 2.08 – 2.01 (m, 2H, -$COOCH_2CH_2$). MS(ESI): 489.53 $[M + H]^+$. Anal. Calcd for $C_{23}H_{25}FN_4O_5S$: C, 56.55; H, 5.16; N, 11.47%; Found: C, 56.76; H, 5.14; N, 11.51.

2-Morpholinoethyl-1-(4-sulfamoylphenyl)-5-(4-(trifluoromethyl)phenyl)-1*H*-pyrazole-3-carboxylate(A32)

White solid, yield 21.1%, m.p. 178.3-178.8 □. ^{1}H NMR (600 MHz, Chloroform-*d*) *δ*: 7.81 – 7.73 (m, 2H, -ArH), 7.63 (d, *J*= 8.2 Hz, 2H, -ArH), 7.42 –

7.36 (m, 2H, -ArH), 7.33 (d, *J*= 8.1 Hz, 2H, -ArH), 7.15 (s, 1H, =CH), 6.72 (s, 2H, $-SO_2NH_2$), 4.53 (s, 2H, $-COOCH_2$), 3.76 (s, 4H, $-CH_2$), 2.85 (s, 2H, $-COOCH_2CH_2$), 2.61 (s, 4H, $-CH_2$). MS(ESI): 525.52 $[M + H]^+$. Anal. Calcd for $C_{23}H_{23}F_3N_4O_5S$: C, 52.67; H, 4.42; N, 10.68%; Found: C, 52.86; H, 4.41; N, 10.64.

_N_-(3-Morpholinopropyl)-1-(4-sulfamoylphenyl)-5-(4-(trifluoromethyl)phenyl)-1 _H_-pyrazole-3-carboxamide(A33)

White solid, yield 51.6%, m.p. 203.6-204.8 □. ^{1}H NMR (600 MHz, DMSO-d_6) δ: 8.64 (t, *J*= 6.0 Hz, 1H, -CONH), 7.93 – 7.87 (m, 2H, ArH), 7.79 (d, *J*= 8.1 Hz, 2H, ArH), 7.60 – 7.49 (m, 6H, ArH, $-SO_2NH_2$), 7.20 (s, 1H, =CH), 3.83 (s, 4H, $-CH_2$), 3.34 (s, 2H, $-CONHCH_2$), 3.01 (m, 5H, -CH2, $-CONHCH_2CH_2CH_2$), 2.73 (s, 1H, $-CONHCH_2CH_2CH_2$), 1.94 (d, *J*= 9.7 Hz, 2H, $-CONHCH_2CH_2$). MS(ESI): 538.56 $[M + H]^+$. Anal. Calcd for $C_{24}H_{26}F_3N_5O_4S$: C, 53.62; H, 4.88; N, 13.03%; Found: C, 53.82; H, 4.86; N, 13.07.

3-Morpholinopropyl-1-(4-sulfamoylphenyl)-5-(4-(trifluoromethyl)phenyl)-1*H*-py razole-3-carboxylate(A34)

White solid, yield 54.2%, m.p. 181.4-182.3 □. ^{1}H NMR (600 MHz, DMSO-d_6) δ: 7.90 (d, *J*= 8.7 Hz, 2H, ArH), 7.80 (d, *J*= 8.3 Hz, 2H, ArH), 7.59 – 7.52 (m, 6H,ArH, $-SO_2NH_2$), 7.32 (s, 1H, =CH), 4.36 (t, *J*= 6.6 Hz, 2H, $-COOCH_2$), 3.57 (t, *J*= 4.6 Hz, 4H, $-CH_2$), 2.41 (t, *J*= 7.1 Hz, 2H, $-COOCH_2CH_2CH_2$), 2.37 (s, 4H, $-CH_2$), 1.88 (p, *J*= 6.8 Hz,2H, $-COOCH_2CH_2$). MS(ESI): 539.54 $[M + H]^+$. Anal. Calcd for $C_{24}H_{25}F_3N_4O_5S$: C, 53.53; H, 4.68; N, 10.40%; Found: C, 53.73; H, 4.67; N, 10.44.

5-(4-Methoxyphenyl)-*N*-(2-morpholinoethyl)-1-(4-sulfamoylphenyl)-1*H*-pyrazole -3-carboxamide(A35)

White solid,yield 22.1%, m.p. 120.3-120.9 □. ^{1}H NMR (600 MHz, DMSO-d_6) δ: 8.23 (t, *J*= 5.9 Hz, 1H, -CONH), 7.89 – 7.85 (m, 2H, ArH), 7.54 (d, *J*= 8.6 Hz, 2H, ArH), 7.50 (s, 2H, ArH), 7.23 (d, *J*= 8.7 Hz, 2H, $-SO_2NH_2$), 6.99 – 6.91 (m, 3H, ArH, =CH), 3.77 (s, 3H, $-OCH_3$), 3.57 (t, *J*= 4.6 Hz, 4H, $-CH_2$), 3.40 (q, *J*= 6.5 Hz, 2H, $-CONHCH_2$), 2.47 (t, *J*= 6.8 Hz, 2H, $-CONHCH_2CH_2$), 2.42 (s, 4H, $-CH_2$). ^{13}C NMR

(151 MHz, DMSO-d_6) δ 161.29, 160.14, 144.91, 143.86, 130.60, 127.15, 126.20, 121.72, 114.76, 108.22, 66.68, 57.82, 55.72, 53.71, 40.52, 36.19. MS(ESI): 486.56 [M + H]$^+$. Anal. Calcd for $C_{23}H_{27}N_5O_5S$: C, 56.89; H, 5.61; N, 14.42%; Found: C, 56.67; H, 5.59; N, 14.37.

3-Morpholinopropyl-5-(4-methoxyphenyl)-1-(4-sulfamoylphenyl)-1*H*-pyrazole-3-carboxylate(A36)

White solid, yield 12.1%, m.p. 167.4-168.7 □. ^{1}H NMR (600 MHz, Chloroform-*d*) δ: 7.86 (d, *J*= 8.3 Hz, 2H, ArH), 7.46 (d, *J*= 8.3 Hz, 2H, ArH), 7.28 (s, 2H, -SO_2NH_2), 7.13 (d, *J*= 8.7 Hz, 2H, ArH), 7.00 (s, 1H, =CH), 6.89 (d, *J*= 8.7 Hz, 2H, ArH), 4.49 (t, *J*= 6.3 Hz, 2H, -$COOCH_2$), 3.87 (s, 3H, -CH_2), 3.84 (s, 3H, -OCH_3), 3.81 (s, 1H, -CH_2), 2.79 (s, 6H, -CH_2, -$COOCH_2CH_2$), 2.19 (d, *J*= 5.0 Hz, 2H, -$COOCH_2CH_2$). MS(ESI): 501.57 [M + H]$^+$. Anal. Calcd for $C_{24}H_{28}N_4O_6S$: C, 57.59; H, 5.64; N, 11.19%; Found: C, 57.81; H, 5.65; N, 11.21.

5-(4-Methoxyphenyl)-*N*-(3-morpholinopropyl)-1-(4-sulfamoylphenyl)-1*H*-pyrazole-3-carboxamide(A37)

Light yellow solid, yield 27.2%, m.p. 168.8-169.4 □. ^{1}H NMR (600 MHz, Chloroform-*d*) δ: 7.89 – 7.83 (m, 2H, ArH), 7.46 (d, *J*= 8.6 Hz, 2H, ArH), 7.28 (s, 2H, -SO_2NH_2), 7.13 (d, *J*= 8.7 Hz, 2H, ArH), 6.98 (s, 1H, =CH), 6.88 (d, *J*= 8.7 Hz, 2H, ArH), 4.47 (t, *J*= 6.5 Hz, 2H, -$CONHCH_2$), 3.84 (s, 3H, -OCH_3), 3.76 (t, *J*= 4.7 Hz, 4H, -CH_2), 2.63 (dd, *J*= 18.5, 11.1 Hz, 6H, -CH_2, -$CONHCH_2CH_2CH_2$), 2.06 (s, 2H, -$CONHCH_2CH_2$). MS(ESI): 500.59 [M + H]$^+$. Anal. Calcd for $C_{24}H_{29}N_5O_5S$: C, 57.70; H, 5.85; N, 14.02%; Found: C, 57.47; H, 5.83; N, 14.04.

5-(4-Ethoxyphenyl)-*N*-(2-morpholinoethyl)-1-(4-sulfamoylphenyl)-1*H*-pyrazole-3-carboxamide(A38)

White solid, yield 30%, m.p. 93.5-94.1 □. ^{1}H NMR (600 MHz, DMSO-d_6) δ: 8.25 (t, *J*= 6.0 Hz, 1H, -CONH), 7.87 (d, *J*= 8.6 Hz, 2H, ArH), 7.57 – 7.47 (m, 4H, ArH,), 7.21 (d, *J*= 8.7 Hz, 2H, -SO_2NH_2), 6.99 – 6.91 (m, 3H, ArH, =CH), 4.04 (q, *J*= 7.0 Hz, 2H, -CH_2CH_3), 3.58 (t, *J*= 4.6 Hz, 4H, -CH_2), 3.40 (q, *J*= 6.5 Hz, 2H,

-CONHCH$_2$), 2.45 (s, 6H, -CH$_2$, -CONHCH$_2$CH$_2$), 1.32 (t, *J*= 7.0 Hz, 3H, -CH$_2$CH$_3$). ^{13}C NMR (151 MHz, DMSO-d_6) δ 148.15, 144.95, 143.85, 142.18, 130.59, 127.43, 127.14, 126.18, 124.80, 119.52, 115.14, 110.19, 108.18, 66.56, 63.67, 57.75, 53.64, 40.52, 36.08, 15.06. MS(ESI): 500.59 [M + H]$^+$. Anal. Calcd for $C_{24}H_{29}N_5O_5S$: C, 57.70; H, 5.85; N, 14.02%; Found: C, 57.91; H, 5.87; N, 14.04.

3-Morpholinopropyl-5-(4-ethoxyphenyl)-1-(4-sulfamoylphenyl)-1*H*-pyrazole-3-carboxylate(A39)

Yellow solid, yield 65.3%, m.p. 193.1-194.0 □. ^{1}H NMR (600 MHz, DMSO-d_6) δ: 7.88 (d, *J*= 8.6 Hz, 2H, ArH), 7.54 – 7.50 (m, 4H, ArH), 7.21 (d, *J*= 8.8 Hz, 2H, -SO$_2$NH$_2$), 7.08 (s, 1H, =CH), 6.95 (d, *J*= 8.8 Hz, 2H, ArH), 4.34 (t, *J*= 6.6 Hz, 2H, -COOCH$_2$), 4.04 (q, *J*= 7.0 Hz, 2H, -CH$_2$CH$_3$), 3.57 (t, *J*= 4.7 Hz, 4H, -CH$_2$),2.41 (t, *J*= 7.1 Hz, 2H, -COOCH$_2$CH$_2$CH$_2$), 2.36 (s, 4H, -CH$_2$), 1.87 (p, *J*= 6.8 Hz, 2H, -COOCH$_2$CH$_2$), 1.32 (t, *J*= 7.0 Hz, 3H, -CH$_2$CH$_3$). MS(ESI): 515.60 [M + H]$^+$. Anal. Calcd for $C_{25}H_{30}N_4O_6S$: C, 58.35; H, 5.88; N, 10.89%; Found: C, 58.57; H, 5.86; N, 10.92.

5-(4-Ethoxyphenyl)-*N*-(3-morpholinopropyl)-1-(4-sulfamoylphenyl)-1*H*-pyrazole-3-carboxamide(A40)

White solid, yield 17.1%, m.p. 104-104.5 □. ^{1}H NMR (600 MHz, DMSO-d_6) δ: 8.49 (t, *J*= 5.8 Hz, 1H, -CONH), 7.87 (d, *J*= 8.6 Hz, 2H, ArH), 7.57 – 7.48 (m, 4H, ArH), 7.21 (d, *J*= 8.7 Hz, 2H, -SO$_2$NH$_2$), 6.97 – 6.91 (m, 3H, ArH, =CH), 4.04 (q, *J*= 7.0 Hz, 2H, -CH$_2$CH$_3$), 3.57 (t, *J*= 4.6 Hz, 4H, -CH$_2$), 3.33 (q, *J*= 7.9, 6.5 Hz, 2H, -CONHCH$_2$), 2.35 (t, *J*= 6.4 Hz, 6H, -CH$_2$, -CONH$_2$CH$_2$CH$_2$CH$_2$), 1.69 (p, *J*= 6.9 Hz, 2H, -CONHCH$_2$CH$_2$), 1.32 (t, *J*= 7.0 Hz, 3H, -CH$_2$CH$_3$). ^{13}C NMR (151 MHz, DMSO-d_6) δ 161.23, 159.41, 148.30, 144.90, 143.82, 142.18, 130.57, 127.09, 126.12, 121.58, 115.12, 108.18, 66.61, 63.66, 56.93, 53.83, 38.63, 38.03, 26.19, 15.05. MS(ESI): 514.61 [M + H]$^+$. Anal. Calcd for $C_{25}H_{31}N_5O_5S$: C, 58.46; H, 6.08; N, 13.64%; Found: C, 58.31; H, 6.10; N, 13.68.

2-morpholinoethyl5-(4-ethoxyphenyl)-1-(4-sulfamoylphenyl)-1*H*-pyrazole-3-carb

oxylate(A41)

White solid, yield 37.8%, m.p. 190.0-190.3 □. ^{1}H NMR (600 MHz, Chloroform-*d*) *δ*: 7.65 (m, 2H, ArH), 7.31 (m, 2H, ArH), 7.19 (s, 1H, =CH), 7.00(m, 2H, -SO_2NH_2), 6.95 (s, 1H, ArH), 6.77 (m, 3H, ArH), 4.48 (s, 2H, -$COOCH_2$), 3.96 (q, *J*= 7.0 Hz, 2H, -CH_2CH_3), 3.73 (m, 4H, -CH_2), 2.84 (s, 2H, -CH_2), 2.61 (s, 4H, -CH_2), 1.35 (t, *J*= 7.0 Hz, 3H, -CH_2CH_3). ^{13}C NMR (151 MHz, DMSO-d_6) *δ* 161.84, 159.53, 145.10, 144.15, 142.02, 130.71, 127.48, 127.23, 126.27, 124.82, 121.15, 119.53, 115.14, 110.22, 110.18, 66.58, 63.69, 62.21, 56.97, 53.85, 40.52, 15.05. MS(ESI): 501.57 $[M + H]^+$. Anal. Calcd for $C_{24}H_{28}N_4O_6S$: C, 57.59; H, 5.64; N, 11.19%; Found: C, 57.81; H, 5.66; N, 11.22.

4.6. Cell culture

Murine melanoma cell line F10, human lungs cell line A549, human cervix cell line HeLa, human breast cancer cell line MCF-7 and human kidney epithelial cell line 293T were cultivated in Dulbecco's modified Eagle's medium (DMEM) containing 10% fetal bovine serum (FBS, BI), 100 U/mL penicillin and 100 μg/mL streptomycin, and incubated at 37 □ in a humidified atmosphere containing 5% CO_2.

4.7. Statistical Analysis

The statistical data were analyzed by using GraphPad Prism 7.0 software. All tests were performed in triplicates. Data were presented as means ± standard deviation. One-way single factorial analysis of variance (ANOVA) was performed to determine statistical significance of the data. The differences were considered significant for *p* values * <0.05, ** <0.01.

4.8. Cell proliferation assay

The anti-proliferative activities of the synthesized compounds against the F10,

A549, HeLa, MCF-7, and 293T cell lines were evaluated by a modified standard (MTT) -based colorimetric assay. Test cell lines were plated on 96-well plates at the density of 1×10^4 / well and incubated for 12 h at 37 ˚C in DMEM complemented with 10% fetal bovine serum. All the test compounds which were dissolved in DMSO were then treated to the cells at 0 μM, 0.1 μM, 1 μM, 10 μM and 100 μM, incubated for 48 h at 37 ˚C under an atmosphere of 5% CO_2. After that, added MTT (5 mg/mL in PBS) to each well and incubated for 4 h. Added 150 μL DMSO to each well and shook it with a shaker. The absorbance (OD 570 nm) was read on an ELISA reader (ELx800, BioTek, USA) with reference of 630 nm. IC_{50} values of compounds were calculated by comparison with DMSO-treated control wells. Three replicate wells were used for each drug concentration. Each assay was carried out three times.

4.9. *In vitro* COX and 5-LOX inhibition assay

The ability of the synthesized compounds to inhibit COX-1 and COX-2 was determined by COX-1/COX-2 ELISA Kit. Based on the detection principle, PGH_2 is produced by the catalysis of cyclooxygenase by arachidonic acid, $PGF_{2\alpha}$ was derived from PGH_2， reduced by stannous oxide and detected by enzyme immunoassay at a wavelength of 450nm. In general, added 10 μL of various concentrations of test compounds to the supplied reaction buffer (960 μL, 0.1 M Tris-HCl pH 8.0 containing 5 mM EDTA and 2 mM phenol) with COX-1 or COX-2 (10 μL) enzyme in the presence of heme (10 μL), then added 10μL of AA (100 μM) solution to the reaction and incubated for 10 min at 37 ℃ under an atmosphere of 5% CO_2. Subsequently, 50 μL of 1M HCl was added to stop the reaction, followed by one-tenth the volume of

855 saturated stannous chloride (50 mg/mL). The reaction mixture was incubated at room
856 temperature for 5 minutes. The plate was washed to remove any unbound reagent and
857 Ellman's reagent containing the acetylcholinesterase substrate was then added to the
858 well. According to the yellow intensity produced by the reaction staining, the enzyme
859 immunoassay was used to determine the wavelength of each well at 450 nm.

860 The inhibitory potency of test compounds on 5-LOX was determined by the
861 production of LTB_4 f which was stimulated by the calcium ionophore A23187,
862 Sprague Dawley rats were injected intraperitoneally with 20 mL/kg of 0.2% (w/v)
863 glycogen solution to obtain Leukocytes from the abdominal cavity. The cell fluid was
864 collected with the Hanks solution and plated it at the density of 2.0×10^5 cells per well
865 in a 24-well. After incubation for 10 min at 37□, L-cysteine (11 mM), indomethacin
866 (1 mg/L), DMSO, Celecoxib and test compounds were added successively to each
867 well and incubated for another 30 minutes. After that, the calcium ionophore A23187
868 (5 mmol) was added to initiate LTB_4 production and incubated for 30 minutes. After
869 clarification by centrifugation, the supernatant was plated into 96-well plates and
870 incubated overnight at 4 □. Added chromogen and it remained for 90 minutes. The
871 5-LOX activity was evaluated using an ELISA kit. 50% Inhibition of the test
872 compounds concentration (IC50, μM) based on concentration inhibition response
873 curves.

874 **4.10. Molecular modeling (docking) study**

875 Structures of the ligands and proteins were both minimized and prepared through
876 the graphical user interface DS-CDOCKER protocol. The three-dimensional X-ray

structure of COX-2 (PDB code: 3LN1) and 5-LOX (PDB code: 3V99) were obtained from the RCSB Protein Data Bank (http://www.rcsb.org/pdb/home/home.do), implemented by Discovery Studio (version 3.5). Removed all bound water and ligand from the protein and added the polar hydrogen to it. At the same time as the protein is being prepared, a given active site is defined as a binding pocket. Molecular docking was to dock the prepared ligand to the binding pocket of COX-2 and 5-LOX based on the binding mode. Each compound will retain 10 poses, be classified according to CDOCKER_INTERACTION_ENERGY. Selected the best pose of these ligands to interact with amino acid residues in the active site. Analyzed the type of interaction between the docking protein and the ligands.

4.11. Analysis of cellular apoptosis

F10 cells were plated in 6-well plates at the density of 1.0×10^6 cells and incubated for 24 h at 37 □, then test compounds were added in a certain concentration and negative control which was treated with medium were included. After 48 hours of incubation, collected trypsin-digested cells, washed twice with PBS and centrifuged at 2000 rpm to collect cells. 500μL of the buffer was added to suspend cells, then added 5μL Annexin V-FITC and 5μL PI in dark conditions. Fully mixed, reacted for 15 minutes at room temperature in dark, and then analyzed the cell apoptosis with the FACSCalibur flow cytometer (Becton Dickinson, San Jose, CA, USA).

4.12. Analysis of cell cycle arrest

F10 cells were plated, treated with test compounds and incubated for 48 hours as described above. Collected trypsin-digested cells were washed twice with PBS and

centrifuged at 2000 rpm to collect cells. 1 mL PBS containing 70% cold ethanol was added to fix cells at 4 □ (overnight). It was centrifuged at 5000 rpm and the supernatant was discarded. After the addition of 100 μL of RNase A, incubation at 37 □ for 30 minutes and addition of 400 μL PI. Cell DNA content was measured using FACSCalibur flow cytometer (Becton Dickinson, San Jose, CA, USA).

4.13. The detection of PGE_2 production

F10 cells were seeded in 6-well plates (2×10^5 cells/well) and incubated at 37 ℃ for 12 h, then replaced the culture medium with fresh medium containing 1 μg /ml LPS to induce PGE_2 expression. Subsequently, the cells were treated with celecoxib (6.25 μM) or compound **A33** (6.25 μM) for 24h. The supernatant was collected by centrifugation at 14,000 ×*g* for 10 minutes at 4°C, and then the production of PGE_2 was measured using the PGE_2 enzyme immunoassay kit (catalog No.514010, Cayman Chemical) according to the manufacturer's instructions.

4.14. *In vivo* antitumor assay

6-8 week-old nude mice were purchased from the Model Animal Research Center of Nanjing University (Nanjing, China) which were fed in a specific pathogen-free environment. F10 cells（5×10^6）in 100μL DMEM were injected subcutaneously into the right flank of the nude mouse (18-22g) to establish the xenograft model. When the tumor mass was visible and the tumor size was close to 100mm^3. The tumor-bearing nude mice were randomly divided into four groups (6 mice/group), the vehicle-treated group, the compound **A33** (20 mg/kg)-treated group, the compound **A33** (40 mg/kg)-treated group, and the **Celecoxib** (20 mg/kg)-treated group. Treated the

vehicle-treated group with polyethylene glycol (containing 1% DMSO). The method of administration was given by intraperitoneal injection, every two days, for 14 days. After the start of dosing, mice were weighed every two days and tumor volume was measured with a Vernier caliper at the same time. After the drug treatment, all mice were executed and the Animal welfare and experimental procedures were carried out in strict compliance with the "Guide for the Care and Use of Laboratory Animals" and the related ethical regulations of Nanjing University.

4.15. Test compound pharmacokinetics in tumor-bearing nude mice

The test compound was administered to tumor-bearing nude mice by the intraperitoneal administration at a dose of 40 mg/kg. After 24 h and 48 h of administration, blood samples were taken from the eyeballs. Blood samples (0.2 mL) were withdrawn to the heparinized Vacutainer tubes and centrifuged at 800 × *g* and 4°C immediately for 4 minutes. A volume of 100 μL of plasma was obtained. The target compound and its raw material in the previous step were selected and dissolved in ethyl acetate to serve as a control group, at the same time, ethyl acetate was selected to extract the drug from plasma. HPLC methods have been used for the analysis of testing samples. The analyses of drug metabolism in mice were performed using a C-18 reverse phase column (Water Symmetry C-18 5 μM, 150mm × 4.6mm). The mobile phase consists of 0.8% triethylamine/acetic acid (*v*/*v*) in a mixture of 20% acetonitrile and 80% water, and the mobile phase flow rate was 1 mL/min. The detection was performed using a fluorescence detector (Shimazu Scientific Instruments Inc., Columbia, MO) with an excitation wavelength of 254 nm.

Acknowledgments

The work was financed by the Nation Nature Science Foundation of China (No.21602103) and Public Science and Technology Research Fund Project of Ocean (No. 201505023).

References:

[1]. Gabriele, M.; Michael, M.; Jürgen, R., Chronic Inflammation in Cancer Development. *Frontiers in Immunology,* **2011,** *2* (2), 1-17.
[2]. Meylan, E.; Dooley, A. L.; Feldser, D. M.; Shen, L.; Turk, E.; Ouyang, C.; Jacks, T., Requirement for NF-kappaB signalling in a mouse model of lung adenocarcinoma. *Nature,* **2009,** *462* (7269), 104-107.
[3]. Mantovani, A.; Allavena, P.; Sica, A.; Balkwill, F., Cancer-related inflammation. *Nature,* **2008,** *454* (7203), 436-444.
[4]. Riemann, A.; Ihling, A.; Reime, S.; Gekle, M.; Thews, O., Impact of the Tumor Microenvironment on the Expression of Inflammatory Mediators in Cancer Cells. *Advances in Experimental Medicine & Biology,* **2016,** *923*, 105-111.
[5]. Meresman, G. F.; Olivares, C. N., *Involvement of prostaglandins in the pathophysiology of endometriosis*. 2012, 116-132.
[6]. Matsuyama, M.; Yoshimura, R., Arachidonic acid pathway: A molecular target in human testicular cancer (Review). *Molecular Medicine Reports,* **2009,** *2* (4), 527-531.
[7]. Zebardast, T.; Zarghi, A.; Daraie, B.; Hedayati, M.; Dadrass, O. G., Design and synthesis of 3-alkyl-2-aryl-1,3-thiazinan-4-one derivatives as selective cyclooxygenase (COX-2) inhibitors. *Cheminform,* **2009,** *345* (4), 3162-3165.
[8]. Maitra, A.; Ashfaq, R.; Gunn, C. R.; Rahman, A.; Yeo, C. J.; Sohn, T. A.; Cameron, J. L.; Hruban, R. H.; Wilentz, R. E., Cyclooxygenase 2 expression in pancreatic adenocarcinoma and pancreatic intraepithelial neoplasia: an immunohistochemical analysis with automated cellular imaging. *American Journal of Clinical Pathology,* **2002,** *118* (2), 194-201.
[9]. Smith, W. L.; Garavito, R. M.; Dewitt, D. L., Prostaglandin Endoperoxide H Synthases (Cyclooxygenases)-1 and −2. *Journal of Biological Chemistry,* **1996,** *62* (52), 33157-33160.
[10]. Ye, Y. N.; Wu, W. K.; Shin, V. Y.; Bruce, I. C.; Wong, B. C.; Cho, C. H., Dual inhibition of 5-LOX and COX-2 suppresses colon cancer formation promoted by cigarette smoke. *Carcinogenesis,* **2005,** *26* (4), 827-834.
[11]. Matsuyama, M.; Yoshimura, R.; Tsuchida, K.; Takemoto, Y.; Segawa, Y.; Shinnka, T.; Kawahito, Y.; Sano, H.; Nakatani, T., Lipoxygenase inhibitors prevent urological cancer cell growth. *International Journal of Molecular Medicine,* **2004,** *13* (5), 665-668.
[12]. Zhao, Y.; Wang, W.; Wang, Q.; Zhang, X.; Ye, L., Lipid metabolism enzyme

5-LOX and its metabolite LTB4 are capable of activating transcription factor NF-κB in hepatoma cells. *Biochemical & Biophysical Research Communications,* **2012,** *418* (4), 647-651.

[13]. Tavolari, S.; Bonafè, M.; Marini, M.; Ferreri, C.; Bartolini, G.; Brighenti, E.; Manara, S.; Tomasi, V.; Laufer, S.; Guarnieri, T., Licofelone, a dual COX/5-LOX inhibitor, induces apoptosis in HCA-7 colon cancer cells through the mitochondrial pathway independently from its ability to affect the arachidonic acid cascade. *Carcinogenesis,* **2008,** *29* (2), 371-380.

[14]. Mutoh, M.; Takahashi, M.; Wakabayashi, K., Roles of prostanoids in colon carcinogenesis and their potential targeting for cancer chemoprevention. *Current Pharmaceutical Design,* **2006,** *12* (19), 2375-2382.

[15]. Prescott, S. M.; White, R. L., Self-promotion? Intimate connections between APC and prostaglandin H synthase-2. *Cell,* **1996,** *87* (5), 783-786.

[16]. Cao, Y.; Pearman, A. T.; Zimmerman, G. A.; Mcintyre, T. M.; Prescott, S. M., Intracellular Unesterified Arachidonic Acid Signals Apoptosis. *Proceedings of the National Academy of Sciences of the United States of America,* **2000,** *97* (21), 11280-11285.

[17]. Reddy, K. K.; Vidya Rajan, V. K.; Gupta, A.; Aparoy, P.; Reddanna, P., Exploration of binding site pattern in arachidonic acid metabolizing enzymes, Cyclooxygenases and Lipoxygenases. *Bmc Research Notes,* **2015,** *8* (1), 1-10.

[18]. Zimmermann, G. R.; Lehár, J.; Keith, C. T., Multi-target therapeutics: when the whole is greater than the sum of the parts. *Drug Discovery Today,* **2007,** *12* (1), 34-42.

[19]. Kurumbail, R. G.; Stevens, A. M.; Gierse, J. K.; Mcdonald, J. J.; Stegeman, R. A.; Pak, J. Y.; Gildehaus, D.; Iyashiro, J. M.; Penning, T. D.; Seibert, K., Structural basis for selective inhibition of cyclooxygenase-2 by anti-inflammatory agents. *Nature,* **1996,** *384* (384), 644-648.

[20]. Abouzid, K. A. M.; Khalil, N. A.; Ahmed, E. M.; El-Latif, H. A. A.; El-Araby, M. E., Structure-based molecular design, synthesis, and in vivo anti-inflammatory activity of pyridazinone derivatives as nonclassic COX-2 inhibitors. *Medicinal Chemistry Research,* **2010,** *19* (7), 629-642.

[21]. Ram, K. V. V. M. S.; Rambabu, G.; Sarma, J. A. R. P.; Desiraju, G. R., Ligand Coordinate Analysis of SC□558 from the Active Site to the Surface of COX□2: A Molecular Dynamics Study. *Journal of Chemical Information & Modeling,* **2006,** *46* (4), 1784-1794.

[22]. Mustafa, G.; Khan, I. U.; Ashraf, M.; Afzal, I.; Shahzad, S. A.; Shafiq, M., Synthesis of new sulfonamides as lipoxygenase inhibitors. *Bioorg Med Chem,* **2012,** *20* (8), 2535-2539.

[23]. Mohammed, K. O.; Nissan, Y. M., Synthesis, molecular docking, and biological evaluation of some novel hydrazones and pyrazole derivatives as anti-inflammatory agents. *Chemical Biology & Drug Design,* **2014,** *84* (4), 473-488.

[24]. Gautam, S.; Rani, S.; Kaithwas, G., Effects of phenidone (Duclox-2/5 inhibitor) against N-methyl-N-nitrosourea induced mammary gland carcinoma in albino rats. *Toxicol Appl Pharmacol,* **2018,** *351*, 57-63.

[25]. Barik, R.; Sarkar, R.; Biswas, P.; Pattnaik, A.; Samanta, S. K.; Manisenthilkumar,

K. T.; Pal, M.; Karmakar, S.; Sen, T., Inhibition of arachidonic acid metabolism and pro-inflammatory cytokine production by Bruguiera gymnorrhiza leaf. *Oriental Pharmacy & Experimental Medicine,* **2013,** *13* (1), 41-49.

[26]. Lee, C. H.; Jiang, M.; Cowart, M.; Gfesser, G.; Perner, R.; Kim, K. H.; Gu, Y. G.; Williams, M.; Jarvis, M. F.; Kowaluk, E. A., Discovery of 4-amino-5-(3-bromophenyl)-7-(6-morpholino-pyridin-3-yl)pyrido[2,3-d]pyrimidine, an orally active, non-nucleoside adenosine kinase inhibitor. *Journal of Medicinal Chemistry,* **2001,** *44* (13), 2133-2138.

[27]. Chrysselis, M. C.; Rekka, E. A.; Siskou, I. C.; Kourounakis, P. N., Nitric oxide releasing morpholine derivatives as hypolipidemic and antioxidant agents. *Journal of Medicinal Chemistry,* **2002,** *45* (24), 5406-5409.

[28]. Ziakas, G. N.; Rekka, E. A.; Gavalas, A. M.; Eleftheriou, P. T.; Kourounakis, P. N., New analogues of butylated hydroxytoluene as anti-inflammatory and antioxidant agents. *Bioorganic & Medicinal Chemistry,* **2006,** *14* (16), 5616-24.

[29]. Pendergrass, K.; Hargreaves, R.; Petty, K. J.; Carides, A. D.; Evans, J. K.; Horgan, K. J., Aprepitant: an oral NK1 antagonist for the prevention of nausea and vomiting induced by highly emetogenic chemotherapy. *Drugs of Today,* **2004,** *40* (10), 853-63.

[30]. Taylor, A. M.; Schreiber, S. L., Aziridines as intermediates in diversity-oriented syntheses of alkaloids. *Cheminform,* **2009,** *40* (42), 3230-323350.

[31]. Sladojevich, F.; Trabocchi, A.; Guarna, A., Stereoselective cyclopropanation of serine- and threonine-derived oxazines to access new morpholine-based scaffolds. *Organic & Biomolecular Chemistry,* **2008,** *6* (18), 3328-3336.

[32]. Qiu, H. Y.; Wang, P. F.; Li, Z.; Ma, J. T.; Wang, X. M.; Yang, Y. H.; Zhu, H. L., Synthesis of dihydropyrazole sulphonamide derivatives that act as anti-cancer agents through COX-2 inhibition. *Pharmacological Research,* **2015,** *104* (7), 86-96.

[33]. Sun, J.; Su, W.; Sheng, G. H.; Lian, Z. M.; Liu, H. Y.; Zhu, H. L., Synthesis of phenylpiperazine derivatives of 1,4-benzodioxan as selective COX-2 inhibitors and anti-inflammatory agents. *Bioorganic & Medicinal Chemistry,* **2016,** *24* (21), 5626-5632.

[34]. Zhu, H. L.; Lu, X. Y.; Wang, Z. C.; Wei, T.; Yan, X. Q.; Wang, P. F., Design, Synthesis and Evaluation of Benzenesulfonamide-substituted 1,5-Diarylpyrazoles containing Phenylacetohydrazide Derivatives as COX-1/COX-2 Agents Against Solid Tumors. *Rsc Advances,* **2016,** *6* (27), 22917-22935.

[35]. Lu, X. Y.; Wang, Z. C.; Ren, S. Z.; Shen, F. Q.; Man, R. J.; Zhu, H. L., Coumarin sulfonamides derivatives as potent and selective COX-2 inhibitors with efficacy in suppressing cancer proliferation and metastasis. *Bioorganic & Medicinal Chemistry Letters,* **2016,** *26* (15), 3491-3498.

[36]. Shen, F. Q.; Wang, Z. C.; Wu, S. Y.; Ren, S. Z.; Man, R. J.; Wang, B. Z.; Zhu, H. L., Synthesis of novel hybrids of pyrazole and coumarin as dual inhibitors of COX-2 and 5-LOX. *Bioorganic & Medicinal Chemistry Letters,* **2017,** *27* (16), 3653-3660.

[37]. Jacob, P. J.; Manju, S. L.; Ethiraj, K. R.; Elias, G., Safer anti-inflammatory therapy through dual COX-2/5-LOX inhibitors: A structure-based approach. *European Journal of Pharmaceutical Sciences,* **2018,** *121,* 356-381.

[38]. Grösch, S.; Tegeder, I.; Niederberger, E.; Bräutigam, L.; Geisslinger, G., COX-2 independent induction of cell cycle arrest and apoptosis in colon cancer cells by the selective COX-2 inhibitor celecoxib. *Faseb Journal*, **2001,** *15* (14), 2742-2744.

[39]. Pelzmann, M.; Thurnher, D.; Gedlicka, C.; Martinek, H.; Knerer, B., Nimesulide and indomethacin induce apoptosis in head and neck cancer cells. *Journal of Oral Pathology & Medicine*, **2010,** *33* (10), 607-613.

1. 41 novel diaryl-1,5-diazoles derivatives bearing morpholine have been synthesized.
2. Their biological activities were evaluated against cancer.
3. Compound **A33** showed the most potent COX-2/5-LOX inhibition.
4. Compound **A33** sufficiently inhibited tumor growth of F10-Xenograft model.